Acta Oncologica Symposium

Image-guided and adaptive radiotherapy

Aarhus - June 5-7, 2008

Final programme
Abstracts

Welcome!

It is our great pleasure to welcome you to Aarhus, Denmark for the 6th Acta Oncologica symposium on image-guided radiotherapy (IGRT).

We look forward to exciting scientific sessions, with presentations from leading scientists from several continents. The meeting has attracted almost 200 physicians, physicists, radiobiologists and other scientists from the Nordic countries and internationally.

All participants and accompanying persons are invited to the social programme. Thursday evening we visit "The Old Town", a national open air museum of urban history and culture in Aarhus city. The tour includes a guided tour and buffet dinner. On Friday night, the conference gourmet dinner will be held at Hotel Marselis.

We hope you will enjoy the meeting and your time in Aarhus - the "city of smile"!

Local organizing committee

Jens Overgaard
Jørgen Petersen
Cai Grau
Morten Hoyer
Jolanta Hansen
Jacob Christian Lindegaard
Ludvig Paul Muren

Sponsors

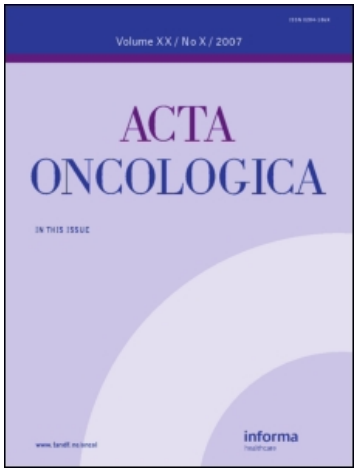

GOLD SPONSORS

VARIAN medical systems

BrainLAB

ELEKTA

SILVER SPONSORS

ACCURAY™

BRONZE SPONSORS

PTW

GE Healthcare

Nucletron

Technical Exhibition

ACCURAY Europe, France

Beampoint AB, Sweden

BrainLAB, Denmark

C-RAD Positioning AB, Sweden

Comecer, Italy

Elekta Instrument AB, Sweden

IBA Dosimetry GmbH

IBA Particle Therapy, Belgium

Limat HB, Sweden

Micropos Medical AB, Sweden

Nucletron Scandinavia AB, Sweden

ORFIT Industries nv, Belgium

Par Scientific A/S, Denmark

PTW-Freiburg AG, Germany

Radeq AB, Sweden

SAM Nordic AB, Sweden

Santax Medico A/S, Denmark

ScandiDos AB, Sweden

Tomotherapy, Hawa-Medical AB, Sweden

Varian Medical Systems Denmark A/S

YourRad AB, Sweden

Aros Art Museum

The Old City

The canal at city centre

Transport

Local bus transport to and from Hotel Marselis: use bus number 6.

Elekta VMAT
– a breakthrough in dose conformance

Elekta VMAT delivers breakthrough dose conformance beyond IMRT. Delivering a precise dose in minutes, Elekta VMAT targets the exact location of the treatment volume, resulting in better avoidance of critical structures and optimal coverage.

Conformance

One or multiple arcs for precise dose control resulting in better avoidance of critical structures.

Speed

Dramatically shorter treatment times than current IMRT techniques.

Ultra-low Dose

Allows daily 3D volumetric imaging and fewer MUs.

Fighting serious disease www.elekta.com

Stereotactic Neurosurgery · Gamma Knife® surgery · Functional Mapping
Precision Radiation Therapy · Image Guided Radiation Therapy · Stereotactic Radiation Therapy

ELEKTA®

exactrac-igrt.com/two

How many minutes does your patient setup take?

ExacTrac® X-Ray 6D offers patient setup in just two minutes. X-ray images are automatically fused with DRRs and patient setup is precisely calculated in a flash, keeping your workflow and throughput on track. ExacTrac X-Ray 6D—one, two…treat.

unlocking possibilities

BrainLAB
oncology solutions

Invited faculty

M Alber (Tübingen)
M Baumann (Dresden)
K Brock (Toronto)
E Brun (Lund)
C Fiorino (Milano)
J Geleijns (Leiden)
K Haustermans (Leuven)
M Kessler (Ann Arbor)
S Korreman (Copenhagen)
G Li (New York)
C Ling (New York)
TR Mackie (Madison)
C Nutting (London)
DR Olsen (Oslo)
R Pötter (Vienna)
A Skretting (Oslo)
V Valentini (Rome)
M van Herk (Amsterdam)
D Verellen (Brussels)
L Østergaard (Århus)

Local organizers

Morten Hoyer
Jens Overgaard
Jacob Christian Lindegaard
Jørgen Petersen
Jolanta Hansen
Ludvig Paul Muren
Cai Grau

Department of Oncology,
Department of Exp. Clinical Oncology,
Department of Medical Physics,
Aarhus University Hospital,
44 Norrebrogade,
DK-8000 Aarhus C
Denmark

Thursday June 5, 2008

2:00 pm – 2:10 pm **Opening of the Symposium**
Cai Grau

2:10 pm – 3:10 pm **Session 1: Basic imaging physics and technology**
Chairperson: Dag Rune Olsen

Recent advances in CT technology
Jacob Geleijns, Leiden, The Netherlands

Applications of PET in radiation treatment planning: Image characteristics and presentation
Arne Skretting, Oslo, Norway

MRI for radiotherapy professionals
Leif Østergaard, Aarhus, Denmark

3:10 pm – 3:30 pm Coffee break

3:30 pm – 4:30 pm **Session 2: Meet the industry**
Chairpersons: Dirk Verellen and Jørgen Petersen

Brainlab
Implementation of image guided radiotherapy using Exactrac with Robotics in Aalborg
Jesper Carl, Aalborg, Denmark

Elekta
Experiences of IGRT, VMAT and hopes for combined INTREPID VMAT
Vibeke Nordmark Hansen, Sutton, United Kingdom

Varian
Bringing the RapidArc technique into clinical practice: First experiences at Rigshospitalet, Copenhagen
Stine Sofia Korreman, Copenhagen, Denmark

4:45 pm – Visit at ”The Old Town”, a national open air museum of urban history and culture, located in Aarhus city. The tour includes a guided tour and buffet dinner. Busses leave in front of hotel at 4:45 p.m. sharp, return at 9-11 pm.

Friday June 6, 2008

8:15 am – 10:45 am **Session 3: Biological imaging**
Chairpersons: C. Clifton Ling and Jens Overgaard

Noninvasive molecular imaging of tumor hypoxia in human xenografts: comparing hypoxia-induced gene expression with endogenous and exogenous hypoxia markers
Gloria Li, New York, USA

Dose painting based on MRI and perfusion imaging
Dag Rune Olsen, Oslo, Norway

Dose painting and optimisation
Markus Alber, Tübingen, Germany
Use of functional imaging for head and neck radiotherapy planning Chris Nutting, London, UK

Functional imaging in rectal cancer
Karin Haustermans, Leuven, Belgium

DCEMRI monitoring of canine tumors during fractionated radiotherapy
Åste Søvik, Oslo, Norway

PET-hypoxia resolution
Morten Busk, Aarhus, Denmark

Treatment planning optimisation based on imaging tumour proliferation and cell density
Alexandru Dasu, Umeå, Sweden

Treatment optimisation based on PET hypoxia
Iuliana Toma-Dasu, Stockholm, Sweden

Dynamic contrast enhanced MRI of bladder cancer and implications for biological image adapted radiotherapy
Kathrine Røe, Oslo, Norway

10:45 – 11:10 am Coffee break

11:10 – 12:20 am **Session 4: Technology for in-room anatomical imaging**
Chairpersons: Claudio Fiorino and Lars Præstegaard

An overview of volumetric imaging technologies and their quality assurance
Dirk Verellen, Brussels, Belgium

Possibilities and challenges in CBCT imaging
Marcel van Herk, Amsterdam, The Netherlands

Tomotherapy
Rock Mackie, Wisconsin, USA

Simulation of CBCT projections
Erik Wåhlin, Stockholm, Sweden

Lunch break

1:15 pm – 2:35 am **Session 5: Image management and registration**
Chairpersons: Rock Mackie and Kari Tanderup

Image Registration for IGRT: Opportunities and challenges
Marc Kessler, Ann Arbor, USA

Integration through registration: Deformable registration for IGRT
Kristy Brock, Toronto, Canada

Accelerating compute intensive image processing in image-guided radiotherapy
Karsten Østergaard Noe, Aarhus, Denmark

Characterisation of radiotherapy planning volumes using textural analysis
William H. Nailon, Edinburgh, UK

An investigation of the accuracy of radiotherapy dose plans calculated on the basis of tissue-segmented CT images
Karsten Eilertsen, Oslo, Norway

A phantom for characterization of geometrical linearity in MR
Tor Arne Vestad, Oslo, Norway

2:35 pm – 3:00 pm Coffee break

3:00 pm – 5:20 pm **Session 6: Clinical studies - pelvis**
Chairpersons: Karin Haustermans and Ludvig Muren

Physics aspects of prostate tomotherapy: planning optimization and image-guidance issues
Claudio Fiorino, Milano, Italy

IGRT in rectal cancer
Vincenzo Valentini, Rome, Italy

Image guided adaptive brachytherapy in cervix cancer
Richard Pötter, Vienna, Austria

Image-guidance protocol comparison: supine and prone setup accuracy for pelvic radiation therapy
Martin Fuss, Portland, USA

Intra-fractional prostate motion and set-up error progression studied by continuous electronic portal imaging
Per Rugaard Poulsen, Stanford/Aarhus, USA/Denmark

A new fiducial marker for image guided radiotherapy of prostate cancer
Jesper Carl, Aalborg, Denmark

A comparison between skin, bone and gold markers for prostate external radiotherapy treatment: Impact on PTV margins
Arve Kylling, Ålesund, Norway

The impact of on-line correction for rotational organ motion in image-guided radiotherapy of the bladder and prostate
Tony Redpath, Edinburgh, UK

Optimal treatment margins for complication-free curative radiotherapy based on interfraction tumor displacement and organ deformation
Eirik Malinen, Oslo, Norway

The normal tissue sparing potential of adaptive strategies in radiotherapy of bladder cancer based on fiducials
Pauliina Wright, Aarhus, Denmark

A dose planning study on applicator guided stereotactic IMRT boost in combination with 3D MRI based brachytherapy in locally advanced cervical cancer
Kari Tanderup, Aarhus, Denmark

Saturday June 7, 2008

8:15 am – 9:35 am **Session 7: Clinical studies - thorax**
Chairpersons: Marcel van Herk and Morten Hoyer

The role of image guidance in respiratory gated radiotherapy
Stine Korreman, Copenhagen, Denmark

Active breath control and in-vivo portal dosimetry for lung tumors
Angelo Piermattei, Campobasso, Italy

Lung and heart dose volume and function study of image guided respiratory gating radiotherapy for left breast cancer treatment using deformable imaging registration
Sean Zhang, Houston, Texas

Can respiratory coaching for 4D CT emulate free breathing during the treatment course?
Gitte Persson, Copenhagen, Denmark

4DCT image-guidance for SBRT
Martin Fuss, Portland, USA

On-line image guidance for stereotactic radiotherapy of lung malignancies by cone beam CT: Comparison Between Target Localization And Alignment On Bony Anatomy
Laura Masi, Florence, Italy

Inter- and intrafractional movement of the tumour in extracranial stereotactic radiotherapy of NSCLC
Carsten Brink, Odense, Denmark

9:35 am – 10:00 am Coffee break

10:00 am – 11:10 am **Session 8: Clinical studies - head-and-neck and brain**
Chairpersons: Martin Fuss and Cai Grau

PET/CT in head and neck oncology
Eva Brun, Lund, Sweden

Salivary gland volume and dose in IMRT for head and neck cancer
assessed using cone-beam CT
Ulrik V. Elstrøm, Aarhus, Denmark

Daily volumetric image-guidance: Does routine usage prompt adaptive re-planning?
James Tanyi, Portland, USA

Setup errors in patients undergoing image guided radiation treatment: Relationship to body mass index and weight loss
Jørgen Johansen, Odense, Denmark

In-vivo portal dosimetry for head-and-neck adaptive IMRT treatment
Savino Cilla, Campobasso, Italy

Clinical results of high-precision cone-beam CT-guided intra cranial stereotactic radiosurgery
Klaus Seiersen, Aarhus, Denmark

11:10 am – 12:00 am

Closing session: The future of IGRT
Chairperson: Jacob Lindegaard

Cost-benefit analysis of IGRT
Michael Baumann, Dresden, Germany

Broadening the Scope of Image-Guided Radiotherapy
C. Clifton Ling, New York, USA

Closing of the Symposium
Cai Grau

Posters - on display throughout the meeting

Evaluation of long-term changes in lung tumors by transit in-vivo dosimetry
Andrea Fidanzio, Roma, Italy

Experience with daily online image guided positioning in radiotherapy
Martin Skovmos Nielsen, Aalborg, Denmark

Multimodality imaging in radiation treatment planning for carcinoma of the nasopharynx: a sub-volume analysis
Allan Fowler, Sydney, Australia

Localization of the prostate in patients with prostate cancer with three different imaging methods
Áshildur Logadóttir, Copenhagen, Denmark

Early clinical experience using implanted fiducial markers and daily online isocenter setup correction in prostate cancer radiotherapy
Ståle Ølberg, Oslo, Norway

Stereotactic body radiotherapy for medically inoperable stage I non-small cell lung cancer: mature outcome and toxicity results
Neil Kopek, Aarhus, Denmark

A video-fluoroscopic analysis of liver respiratory motion using fiducial markers to measure effectiveness and reproducibility of motion reduction by abdominal compression
W. Wunderink, Rotterdam, The Netherlands

Gated radiotherapy of lung cancer: interfractional changes in tumor volume and position during the treatment course
T. Juhler-Nøttrup, Copenhagen, Denmark

Three-dimensional set-up errors assessment in post-operative head and neck radiotherapy using electronic portal imaging device
J.P. Agarwal, Mumbai, India

Recent advances in CT technology

Geleijns J. Radiology Department, Leiden University Medical Center, Leiden, The Netherlands

CT scanning in a laboratory setting was introduced in 1971 followed in 1974 by 60 clinical installations of CT head scanners. In 1976 CT body scanners became available and technology such as multisource and multislice CT with three x-ray tubes and three detector rows was described already in 1980. In the same year a CT scanner with 14 x-ray tubes and 14 image intensifiers was installed in the Mayo clinic. Main achievements in 1980 were that all basic scientific concepts for CT were developed and tested. But there was no prospect yet of large scale clinical implementation of advanced CT technology. Recent developments are breakthoughs in CT engineering include spiral CT acquisitions with a rotating fan shaped X-ray beam and detector and simultaneous table translation in 1989. Multislice CT scanners were introduced in 1998 (4-detector row scanner) followed by 16-detector row CT in 2001 and 64-detector row CT in 2004. One manufacturer introduced in 2005 a dual source CT scanner in 2005 equipped with two x-ray tubes, and two detectors. Another manufacturer introduced in 2007 volume CT with a 320 detector row volume CT scanner and a coverage of 160mm. Wide bore multislice CT delivering more precision in radiotherapy planning was introduced in 2003. Prospective triggered and retrospective gated techniques for cardiac and lung imaging enhanced the performance of the modern CT scanners. CT guided biopsy and intervention is a relatively new application. Current and future developments include the introduction of dual energy CT with the promise of more specific tissue characterization and better discrimination of iodine enhanced vessels, collagen and bone structures. Breast CT is developed as a new screening technology that may be able to detect tumors earlier than mammography, it is now being tested in patients. CT perfusion offers new opportunities in acute stroke and oncology imaging (e.g. tumor perfusion imaging). CT screening of asymptomatic individuals is investigated in clinical research studies and may be beneficial for lung cancer screening in smokers of particular ages, CT virtual colonoscopy is considered as an alternative for colonoscopy screening in men and women over 50 years of age and CT coronary calcium scoring for predicting heart disease.

Applications of PET in radiation treatment planning: Image characteristics and presentation

Arne Skretting, Department of Medical Physics, Rikshospitalet Medical Centre, Oslo, Norway

The quality of PET images is affected by the spatial resolution power which mainly depends on the detector geometry and by the parameters chosen for the reconstruction: number of iterations, image format and width of any smoothing filter applied during reconstruction. The spatial resolution is of the order of 5 mm full width at half maximum (FWHM). It is possible to characterize the properties of the PET scanner by phantom studies and some examples will be presented. A crucial point in the application of PET images in radiotherapy planning is how the tumour volume should be determined, and examples of different techniques will be shown. The delineation challenge is generally manageable when the radionuclide uptake is homogeneous and the tumour volume is large and regular. When the tumour volume becomes small or very irregular, delineation gets difficult and there is no clear cut strategy. In these situations, thin parts of the tumour loose image intensity and simple techniques like isointensity contouring will not work. Examples will be presented of work carried out in our institution to investigate these phenomena by the use of phantoms made from a fast-settling gel that contain both uniformly distributed ^{18}F and iodine contrast medium. The latter component enables exact determination of the tumour volume and contour from CT image series. Different ways of presenting the PET information together with the CT-information during the planning process will be demonstrated.

Implementation of Exactrac with Robotics in Aalborg

Jesper Carl, Department of Medical Physics, Aalborg Hospital, Aalborg, Denmark

The radiotherapy department in Aalborg is equipped with five linacs and treatment planning system, all from Varian. Department strategy is to have identical linacs. This ensures that patients may be shifted between linacs in order to have an optimized patient flow in the department. From January 2007 and until October 2008 all linacs are being equipped with the Exactrac system including Robotics from Brainlab for image guided radiotherapy. The presentation will focus on the implementation process and the problems encountered. This includes an overview of the system, commissioning and QA, education and training of staff, definition of patient groups and strategies for imaging. A special issue in the system overview is network connection. Exactrac is not a true client server system. Daily work flow, however may be greatly facilitated if all patient data are stored on a common file server. In this case patients can be moved freely between linacs without no need to import patients on each individual linac. Important to the workflow is also remote logon licences which give supervising staff instant remote access to any of linacs in case of problems with the system or image matching. As the use of the linac systems intensify the use of Remote Edit and Review stations are invaluable in order to import patients as part of the planning process, and for retrieving data for statistics or research purposes. Experience and training are critical as will be demonstrated from specific case-wise image matching problems encountered. Finally a more general issue concerning increased attenuation and excess skin dose from new types of carbon fiber imaging couches will be touched upon.

Experiences of IGRT, VMAT and hopes for combined INTREPID VMAT

Hansen VN, Bedford J, Aitkins A, Brock J, Brooks C, Hawkins M, Lalondrelle S, McNair H, and Warrington A.P. Royal Marsden NHS Foundation Trust Downs Road, Sutton, Surrey, SM2 5PT, U.K.

For decades, Radiotherapy practice has involved, to a greater or lesser extent, Image Guided Radiotherapy (IGRT). However, recent technological developments in image guidance on treatment machines is reaching it's full potential with the increasing soft tissue image quality of the latest linac based CT systems, along with wider applications of the more mature MV imaging systems. Both modalities have interesting prospects for further development in the future.
In our hospital, we have recently commissioned five new Elekta Synergy linacs equipped with both IviewGT, for the acquisition of MV images, and XVI CT systems. In addition a Philips Brilliance Large Bore CT scanner capable of 4D CT data acquisition has been installed.
Using the 4DCT scanner we are able to fully appreciate lung tumour motion both for increased accuracy in tumour outlining, and also to assess the potential benefit of Active Breathing Control (ABC) in individual patients.
For verification of the correct treated volume XVI gives a full 3D volume view of the tissue around the isocentre. This information can be used to correct set up errors and perform adaptive radiotherapy. We are currently investigating the use of different adaptive planning methods in the treatment of bladder and oesophageal cancers.
Within the last year we have started to explore the potential of Volumetric modulated Arc Therapy (VMAT). The plan optimisation is performed with an in-house inverse planning system "AutoBeam" and a final dose calculation is performed on our clinical treatment planning system, Pinnacle3.
Verification measurements of complete VMAT patients have been performed both with film and using the Delta4 QA device (Scandidos AB, Sweden) and our first clinical case was treated in January 2008.
Finally, the inclusion of both XVI CT and INTegrating Rotational EPID dose maps in Volumetric Modulated Arc Therapy (INTREPID VMAT) will be discussed as an interesting objective for future work.

Bringing the RapidArc technique into clinical practice: First experiences at Rigshospitalet, Copenhagen

Stine Korreman, Joakim Medin, Flemming Kjær-Kristoffersen, Lars Ohlhues and Svend Aage Engelholm, Department of Radiation Oncology, Rigshospitalet, Copenhagen University Hospital

Recently, Varian Medical Systems have introduced the new treatment technique, RapidArc™, in which dose is delivered over a single gantry rotation with dynamically varying MLC positions, dose rate and gantry speed. This technique was released for clinical use in late April 2008, and installed at Rigshospitalet, Copenhagen University Hospital, as the first clinic in Europe in early May 2008. Treatment using the technique was started up for prostate cancer patients in early May 2008 immediately after installation.
We here report our experiences with bringing the technique into routine clinical practice. From installation and acceptance, through patient selection, treatment planning and quality assurance, to the actual treatment of prostate cancer patients.
The quality assurance programme has shown that delivery of RapidArc™ treatment plans is consistent with the dose calculated in the treatment planning system, Eclipse 8.5, and that there is high reproducibility of consecutive delivery within the same day and from day to day.
We have also demonstrated that the RapidArc™ treatment technique can be used advantageously in the radiation treatment of prostate cancer patients compared to five-field IMRT. The RapidArc™ treatment plans gave better sparing of organs at risk, in most cases smaller amount of monitor units, and good target homogeneity. Delivery of the RapidArc™ prostate cancer treatment plans can be performed 4-5 times faster than for a five-field IMRT technique using the same linac.

Noninvasive molecular imaging of tumor hypoxia in human xenografts: comparing hypoxia-induced gene expression with endogenous and exogenous hypoxia markers

Gloria C. Li, Ligang Xing, Fuqiu He, Jason A Koutcher and C Clifton Ling. Department of Medical Physics and Department of Radiation Oncology Memorial Sloan-Kettering Cancer Center, New York, USA

Tumor hypoxia is important in the development and treatment of human cancers. We have developed a novel xenograft model for studying and imaging of hypoxia-induced gene expression. A hypoxia-inducible dual reporter HSV1-TKeGFP controlled by 9HRE (hypoxia response element), was stably transfected into human colorectal HT29 cancer cells. Fluorescent microscopy, FACS, and radioactive substrate trapping assays showed strong hypoxia-induced expression of eGFP and TK enzyme in the transfected cells in vitro. Sequential microPET imaging of tumor-bearing mice, using a hypoxia tracer 18F-FMISO and the reporter substrate 124I-FIAU, yielded similar tumor hypoxia images for the HT29-9HRE tumors, but not in the parental tumor. Using autoradiography and IHC, detailed spatial distributions in tumor sections were obtained and compared for various hypoxia biomarkers. Intratumoral distributions of 124I-FIAU and 18F-FMISO were similar, and eGFP, pimonidazole, EF5 and CA9 co-localized in the same areas that were non-perfused. In enabling the detection of hypoxia-induced molecular events and mapping their distribution in vivo with serial noninvasive PET imaging, and multiple parameter analysis with IHC and fluorescence microscopy, this model provides a valuable tool for studying tumor hypoxia and in validating existing and future exogenous markers for tumor hypoxia. Increased expression of cytosine deaminase (CD) and uracil phosphoribosyl-transferase (UPRT) may improve the antitumoral effect of 5-FU and 5-FC. Recently, we are establishing cell lines and developing xenograft models in which CD/UPRT/mDsRed and/or TK/eGFP are placed under the control of a CMV or HRE promoter. The expression/function of the fusion protein is evaluated by FACS, fluorescence microscopy, Western analysis and 5-FU and 5-FC cytotoxicity. In vivo 19F MRS is used to monitor the conversion of 5-FC to 5-FU in CD/UPRT tumors. Pilot 19F MRS studies showed rapid conversion of 5-FC to 5-FU with subsequent anabolism to cytotoxic fluronucleotides (FNucs), with CD/UPRT/mDsRed being more efficient. These models will be valuable for multi-modality molecular and functional imaging studies of tumor hypoxia (PET, MRS, optical), and for monitoring and assessing the efficacy of gene-directed enzyme prodrug therapy.

Dose painting based on MRI and perfusion imaging

Dag Rune Olsen, Eirik Malinen, Åste Søvik. Institute for Cancer Research, Norwegian Radium Hospital, Rikshospitalet University Hospital, University of Oslo, Oslo, Norway

Purpose: Contrast enhanced dynamic MR imaging (ced-MRI) may be used to estimate perfusion and the extracellular–extravascular volume in solid tumours and may potentially be used as a surrogate marker for invasive oxygenation measurements. As such ced-MR imaging may provide relevant information for biological adapted radiation therapy or 'dose paiting' of hypoxic tumours. The purpose of this works has been to explore the possibilities for utilizing ced-MR imaging for dose redistribution and dose distribution optimization in hypoxic solid tumours.
Materials and methods: Ced-MR images of spontaneous canine tumours were subjected to kinetic analysis. Tracer concentration was assumed to be related to tumour oxygenation and comparison with invasive pO_2 measurements were performed for a subset of tumours. Based on oxygenation-related maps derived from the ced-MR images of the tumour different target volume compartments were defined and DICOM structure sets created. Dose redistribution to these compartments was constrained by keeping the average dose to the tumour equal to a conventional target dose. The compartmental doses yielding optimum tumour control probability (TCP) were used as input in an inverse planning system.
Results: The limited comparison between tumour oxygenation based on ced MRI and invasive pO_2 measurements indicated that ced MR imaging may provide representative information about tumour oxygenation. However, before solid conclusions can be drawn a more comprehensive analysis must be undertaken.
Dose re-distribution, resulting from the inverse planning, gave a considerable increase in TCP as compared to uniform distribution of dose. Simulation of random and systematic errors in the oxygen -related images demonstrated reduced TCP for the non-uniform dose prescription. The gain in TCP by dose re-distribution was also shown to depend on tumour reoxygenation as well as on the fraction of transient vs. chronic hypoxic regions.
Conclusions: Improved tumour control may be expected in solid, hypoxic tumours by dose redistribution by inverse planning and IMRT based on ced-MR imaging.

Use of functional imaging for head and neck planning

Christopher Nutting, Royal Marsden Hospital Fulham Road London SW3 6JJ

Tumours in the Head and Neck region are readily immobilized by simple mask or frame systems and for the most part internal organ motion in the Head and Neck region is minimal. The role therefore of image guided radiotherapy for head and neck cancers is predominantly in determining more accurate target volume. CT scanning currently remains the gold standard for identification of tumour and organ at risk and international guidelines are now available for the localization of elective lymph node targets in the neck. MRI scan can be fused with planning CT scans for added accuracy of target volume definition. This is of particular relevance in tumours of the skull base and base of tongue as well as for the identification of organs at risk such as the optic chiasm, which are poorly visualized on CT. Molecular imaging techniques such as FDG PET have been used to identify sub-volumes within the tumour and a number of radioisotopes have been evaluated for localization of areas of tumour hypoxia and tumour proliferation. Clinical data on dose escalation of sub-volumes based on these imaging techniques is emerging. For the imaging of hypoxia, competing techniques include dynamic contrast enhanced MRI and dynamic CT. Data will be presented on our correlative study between these imaging modalities and pathological specimens taken from patients at surgery. Issues of reproducibility of these imaging techniques and stability of areas of hypoxia and proliferation during the course of radiotherapy remain to be evaluated further.

Biological image-guided radiotherapy in rectal cancer: is there a role for FMISO or FLT, next to FDG?

Sarah Roels[1], M.D., Pieter Slagmolen[2], Ir, Johan Nuyts[3], Ir, Ph.D., John A. Lee[4], Ir, Ph.D., Dirk Loeckx[2], Ir, Ph.D., Frederik Maes[2], Ir, Ph.D., Sigrid Stroobants[3], M.D., Ph.D., Freddy Penninckx[5], M.D., Ph.D., Karin Haustermans[1], M.D., Ph.D.

[1]Leuven Cancer Institute, Radiation Oncology, University Hospital Leuven, Leuven, Belgium; [2] Medical Image Computing, ESAT/Radiology, Katholieke Universiteit Leuven, Medical Imaging Center, Leuven, Belgium; [3]Nuclear medicine, University Hospital Leuven, Leuven, Belgium; [4]Center for Molecular Imaging and Experimental Radiotherapy, Université Catholique de Louvain, Brussels, Belgium; [5]Abdominal Surgery, University Hospital Leuven, Leuven, Belgium

Purpose: The purpose of this study is to investigate the feasibility of integrating multiple imaging modalities for image-guided dose-escalation radiation therapy in rectal cancer.
Materials and methods: MRI and PET/CT were performed before, during and after preoperative chemoradiotherapy (CRT) in 15 patients with resectable rectal cancer. PET signals were segmented with an adaptive threshold-based and a gradient-based method. MR TV were manually delineated. A non-rigid registration algorithm was applied to register the MR images to the corresponding PET/CT. Mismatch analyses were carried out to quantify the overlap between MR images and FDG and between FDG and FLT or FMISO tumour volumes (TV) and between PET TVs over time.
Results: The mean MRI and FDG-PET TVs showed a tendency to shrink during and after CRT. in general, the MR TV was larger than the FDG-PET TV on each measured time point. There was a mean 47% mismatch of the FDG TV (15,5 cc) to the corresponding MRI TV (27 cc) at baseline and a 53% mismatch during CRT. During CRT, on average 61% of the FDG TV (7 cc) remained inside the FDG contour at baseline. Similarly, 76% of the MRI TV (13 cc) during CRT overlapped with the baseline TV. FDG-PET TVs delineated with the gradient-based method matched closest with the pathological TV. The mean FDG, FLT and FMISO-PET TVs showed a tendency to shrink during preoperative CRT. On each time point, the mean FDG-PET TV was significantly larger than the FMISO-PET TV, but not significantly larger than the mean FLT-PET TV. There was a mean 65% mismatch between the FMISO and FDG TV obtained before and during CRT. FLT TVs corresponded better with the FDG TVs (25% mismatch before and 56% during CRT). During CRT, on average 61% of the FDG TV (7 cc) overlapped with the baseline TV (15,5 cc). For FLT, the TV overlap was 49% and for FMISO only 20% of the TV during CRT (2 cc) remained inside the contour at baseline (5cc).
Conclusion: Integration of MRI and FDG-PET into the RT planning seems feasible. Gradient-based segmentation is recommended for TV delineation on FDG-PET. FDG, FLT and FMISO-PET reflect different functional characteristics that change during CRT in rectal cancer. FLT and FDG show good spatial correspondence, while FMISO seems less reliable.

DCEMRI monitoring of canine tumors during fractionated radiotherapy

Søvik Å, Skogmo HK, Olsen DR, Malinen E, Department of Radiation Biology, Rikshospitalet, Oslo / Department of Companion Animal Clinical Sciences, The Norwegian School of Veterinary Science, Oslo / Department of Medical Physics, Rikshospitalet, Oslo, Norway

Purpose: To monitor the contrast enhancement in spontaneous canine tumors during fractionated radiotherapy by Dynamic Contrast Enhanced Magnetic Resonance Imaging (DCEMRI).
Methods and Materials: Six dogs with tumors in the oral or nasal cavity received fractionated conformal radiotherapy with 54 Gy given in 18 fractions. T1 weighted DCE imaging was performed prior to each treatment fraction. The tumor was manually delineated in the MR images following every imaging session, and the time dependence of the Relative Signal Increase (RSI) in the tumor was extracted voxel by voxel. RSI images (7 minutes post injection) were generated, in addition to images of the initial slope of the RSI curves. The dependence of the median RSI and median slope in the tumor on the accumulated radiation dose was investigated, and images obtained at different treatment fraction were compared by correlation analysis.
Results: Five out of the six tumors regressed during treatment. The dose dependence of the median RSI varied between the tumors, with some showing an increase and others a decrease in RSI with dose. This was also the case for the initial slope of the RSI curves. For three out of six tumors, the correlation between images acquired before the first treatment fraction and subsequent fractions decreased strongly with accumulated radiation dose.
Conclusions: Large individual variations in the dose response of tumor contrast enhancement were found. Decreasing image correlation resulted both from tumor regression and intratumoral changes in the RSI distribution during treatment. These findings may have consequences for treatment design in biologically adapted radiotherapy.

PET-hypoxia resolution

Busk M[1], Horsman MR[1], Jakobsen S[2], Bussink J[3], van der Kogel A[3] and Overgaard J[1]. [1]Department of Experimental Clinical Oncology, Aarhus University Hospital (AUH), Aarhus, Denmark; [2]PET centre, AUH; [3]Department of Radiation Oncology, Radboud University Nijmegen Medical Centre, Nijmegen, the Netherlands.

Introduction: PET allows non-invasive detection and mapping of tumor hypoxia, which may guide IMRT. However, the combination of slow oxygenation-dependent tracer retention, slow clearance of unbound tracer from non-hypoxic tissue and the necessity to average signal over large non-homogenous tissue areas when applying low resolution PET remains problematic. In this study, we analyze these confounding factors in a tumour model, specifically focusing on the probability of missing foci of hypoxic therapy-resistant cells as a function of tracer equilibration time and voxel/pixel size.
Materials and methods: Murine-derived SCCVII squamous cell carcinomas were grown in mice. Prior to sacrifice mice were injected with fluoroazomycin arabinoside (FAZA, a second-generation PET hypoxia-tracer), and pimonidazole (an immunologically-detectable hypoxia-marker). Tumors and non-hypoxic reference tissue (muscle, blood) were harvested 30, 120 and 240min after FAZA administration. Tumors were halved and, together with blood and muscle, analyzed for radioactivity or frozen and cut. Consecutive sections were analyzed for the distribution of radioactivity (autoradiography) and pimonidazole-adducts and vessels (immunofluorescence microscopy) or necrosis (HE staining).
Results/Discussion: Bio-distribution data revealed that there was no apparent hypoxia-specificity 30 min after FAZA administration. However, tumor-to-reference tissue (muscle, blood) ratios increased dramatically with time reaching values of 2 and 6 when tracer distribution time was prolonged to 2 and 4h, respectively. Results form ongoing image analysis will be presented at the meeting and includes: (i) time-dependent development of intratumoral FAZA contrast and its spatial correlation with pimonidazole; (ii) estimated accuracy of pixel-by-pixel hypoxia-assessment as a function of tracer equilibration time, pixel size and underlying tissue architecture (necrosis, vessels, cell density).

Treatment planning optimisation based on imaging tumour proliferation and cell density

Alexandru Dasu, Department of Radiation Physics, Norrland University Hospital, 901 85 Umeå, Sweden

Functional imaging could provide valuable information on the distribution of biological factors that influence the outcome of radiation therapy. Tumour proliferation and cell density in particular could be imaged with dedicated metabolic tracers and could thus be used for the biological optimisation of treatment plans. The feasibility of individualising treatment planning using proliferation and density information has been investigated through simulations of heterogeneous tumours taking into account the cell density and proliferation rates. The predicted outcome was used to estimate the success of the individualisation of dose distributions. The results have shown that tumour control could be increased through the escalation of doses to proliferating foci with a relative reduction of doses to slowly proliferating regions of the tumour. This suggests that individualisation of treatment planning taking into account proliferation information creates the premises for further reduction of the doses to the surrounding regions which would consequently lead to an increased sparing of the normal tissues. Cell density has been shown to be another important factor that could be used for optimisation, albeit of a lower weight than proliferation. However, associated with proliferation it could lead to treatment failure if the trouble foci are underdosed. In conclusion, treatment optimisation based on imaged proliferation could improve both tumour control and normal tissue sparing.

Treatment optimisation based on PET hypoxia

Toma-Dasu I[1], Uhrdin J[2], Daşu A[3] and Brahme A[1] [1]Stockholm University and Karolinska Institutet, Department of Medical Radiation Physics, 171 76 Stockholm, Sweden, [2]RaySearch Laboratories AB, Sweden, [3]Norrland University Hospital, Department of Radiation Physics, 901 85 Umeå, Sweden

Introduction: Clinical imaging of tumour oxygenation with PET is now possible with several markers and the information obtained could be used to target the potentially troublesome hypoxic foci as hypoxia is an important microenvironmental factor that correlates with treatment failure. This study proposes a simple method to optimize treatment plans based on the conversion of PET hypoxia images into radiosensitivity maps from the uptake properties of the tracers used.
Methods and Materials: PET images were simulated for tumours with heterogeneous oxygenations and then used to calculate the dose distributions using different treatment approaches. Dynamic variations of the hypoxic pattern during fractionated treatments were also simulated in order to estimate the efficiency of each optimisation approach on treatment outcome.
Results: The theoretical approach has been implemented into a treatment planning system that optimises IMRT plans. The results have shown that individualisation of the treatment based on PET imaging of tumour hypoxia could lead to improved treatment outcome while creating the premises for dose reduction in the surrounding normal tissues. The efficiency of including such information into treatment planning is however critically dependent on the approach used to calculate the dose distribution as variations of tumour hypoxia throughout the treatment could lead to considerable loss of control when there are mismatches between planned dose distribution hotspots and acutely varying hypoxic regions. However, automatic approaches for dose prescription have been developed to account for dynamic effects of oxygenation.
Conclusions: Radiation delivery can be optimized based on PET-CT imaging and could lead to significantly improved treatment outcome. In particular hypoxia dynamics has to be taken into consideration in the treatment plan optimization and in the evaluation of the treatment response.

Dynamic contrast enhanced MRI of bladder cancer and implications for biological image adapted radiotherapy

Røe K[1], Muren LP[2], Rørvik J[3], Olsen DR[1], Dahl O[4], Bakke A[5], Malinen E[6]
[1]Dep. Radiat. Biol., Rikshospitalet, Oslo, Norway, [2]Dep. Med. Phys., Aarhus Hosp., Aarhus, Denmark, [3]Dep. Radiol., Haukeland Hosp., Bergen, Norway, [4]Dep. Oncol., Haukeland Hosp. [5]Dep. Urol., Haukeland Hosp. [6]Dep. Med. Phys., Rikshospitalet

Purpose: To assess the role of image parameters derived from dynamic contrast enhanced MRI in bladder cancer staging, and to investigate the potential use of such parameter images in biological image adapted radiotherapy.
Materials and methods: Dynamic Contrast Enhanced (DCE) isotropic volumetric MR images of 1.25 mm resolution were acquired for 27 patients with bladder cancer. DCEMRI parameters derived from tumor and muscle contrast uptake curves were extracted and subjected to correlation analysis with tumor volume as well as clinical, pathological, histological and T2 weighted MR tumor stage. For parameters showing a significant correlation with tumor stage, 3D malignancy maps were generated. For optimal radiotherapy, it was hypothesized that the malignancy map could be used as a biological dose prescription map. To simulate adapted step-and-shoot IMRT using multi-leaf collimators (MLCs), idealized dose distributions, constituted by dose cubes, were adapted to the prescription map. The size of the dose cubes were varied between 2.5 and 10 mm, so as to mimic MLCs of varying leaf width. The difference between the adapted and prescribed dose distributions was estimated by the root mean square deviation (RMSD).
Results: Among the estimated image parameters, only the area between the curves (ABC) for the tumor and for muscle evaluated from 0-480 s (ABC480) correlated significantly with tumor stage ($p=0.04$). The ABC taken at 0-90 s and 0-180 were close to being significant ($p=0.08$ and $p=0.07$, respectively). 3D dose prescription maps for 10 patients were generated from the ABC480. The RMSD between the prescribed and adapted dose distribution increased with increasing size of the dose cubes. Large interpatient variations in the RMSD and in the dependence of the RMSD on different dose cube sizes were found.
Conclusions: The ABC480 may give added value in staging of bladder cancer. High resolution IMRT is required for some patients for optimal adapted radiotherapy.

An overview of volumetric imaging technologies and their quality assurance

Verellen D, De Ridder M, Tournel K, Linthout N, and Storme G, Radiotherapie, Oncologisch Centrum, UZ Brussel, Brussels, Belgium

Image-guided radiation therapy (IGRT) aims at frequent imaging in the treatment room during a course of radiotherapy, with decisions made on the basis of imaging. The concept is far from new, but recent developments and clinical implementations of IGRT drastically improved the quality of radiotherapy and broadened its possibilities as well as its indications. In general IGRT solutions can be classified in planar imaging (e.g. electronic portal imaging devices (EPID) and multiple x-ray source detector systems), volumetric imaging using ionising radiation (kV- and MV- based CT) or non-radiographic techniques (e.g. ultra sound, implanted radiofrequency transponder or MRI). This review will focus on volumetric imaging techniques applying ionising radiation and their appropriate QA for clinical implementation. By far the most important advantage of volumetric IGRT solutions is the ability to visualize soft tissue prior to treatment and defining the spatial relationship between target and organs at risk. A major challenge is imaging during treatment delivery. Planar imaging solutions on the contrary, offer the possibility for real-time imaging during treatment and the potential for tumour tracking, but suffer from the limitation that in general some kind of surrogate is required to locate the target volume (bony structures or implanted radio-opaque markers). As some of these systems consist of peripheral equipment and others present fully integrated solutions, the QA requirements will differ considerably. It should be noted for instance that some systems correct for mechanical instabilities in the image reconstruction process whereas others aim at optimal mechanical stability, and the coincidence of imaging and treatment isocentre needs special attention. Some of the solutions that will be covered in detail are: (a) A high-end diagnostic CT-scanner inside the treatment room. (b) Peripheral systems mounted to the gantry of the treatment machine to acquire cone beam volumetric CT data (CBCT). Both kV-based solutions using an orthogonally mounted kV imaging system or MV-based solutions using EPIDs will be covered. (c) Integrated systems designed for both IGRT and treatment delivery. The helical tomotherapy (TomoTherapy Inc.) approach is such an example where the concept of a binary collimator for helical tomotherapy delivery has been combined with helical CT-scanning obtaining a 2-in-1 concept. This overview will explain some of the technical features and clinical implementations of these technologies as well as providing an insight in the QA-procedures required for each specific solution.

Cone beam CT technology for image guided radiotherapy

Marcel van Herk, National Cancer Institute, AvL Amsterdam, The Netherlands

To account for geometrical uncertainties during radiotherapy, safety margins are applied. In many cases, these margins overlap organs at risk thereby limiting dose escalation. The aim of image-guided radiotherapy is to improve the accuracy by imaging tumor and critical structures on the machine just prior to irradiation. NKI collaborated in the development of a kV cone beam CT guided accelerator. The imaging dose for cone-beam CT is flexible and can be tuned to trade-off image quality, dose, and acquisition speed. Soft tissue guidance of the prostate is the most demanding task, for which we selected 3 cGy imaging dose and 1 min. acquisition time (650 projections). When bony anatomy localization is sufficient, much lower doses can be selected. We use 1 cGy for head and neck with a 35 s scan time (half rotation). However, this dose could easily be lowered for localizing bone. We do not feel the need to do this as the additional imaging dose is already negligible compared with the integral dose delivered by the IMRT technique. For lung, a 4D scanning technique was developed, that is based on sorting projection images on respiratory phase. This technique uses 2 cGy dose, but a long scan time of 4 min to acquire enough respiratory phases. Using deformable cone beam reconstruction, a scan time of 1 minute can probably be achieved in the near future (works in progress). For all our protocols, cone beam reconstruction works concurrent with image acquisition and completes within seconds after scanning. In addition, registration software is integrated in the system's software. The availability of high quality tomographic images and automatic image registration on the machine leads to many new clinical applications, such as high precision hypofractionated treatments of brain metastases and solitary long tumors with on-line tumor position corrections. Adaptive radiotherapy (ART) of prostate cancer is now also in routine use. We adapt to the average prostate and rectum using cone beam scans made during the first week of treatment. The prostate is located automatically in 85% of prostate scans. Even though we use laxatives, the main confounding factor is short-term mobility due to moving gas that causes streak artifacts in the CT reconstructions. It is however, possible to reduce the artifacts by selectively suppressing those projection images where the largest gas motion occurs. Our ART protocol allows reducing the margin from 10 to 7 mm. Patient localization with 1 mm accuracy (bony anatomy) is easily achieved with the current equipment. Pre- and post-treatment scans demonstrate negligible motion of about 0.5 mm SD, both for brain and bladder cancer patients. In conclusion, the availability of cone beam CT on the linear accelerator makes ART very efficient and more accurate, since problem duplicating the setup on the CT scanner are avoided. For all image-guided protocols, the residual uncertainties need to be taken into account, and the safe level of margin reduction evaluated.

Simulation of CBCT projections

Wåhlin, E, Panettieri, V. and Lax, I. Department of Hospital Physics, Karolinska University Hospital, Stockholm, Sweden

Introduction: As part of a large research programme on stereotactic body radiation therapy (SBRT), this work aims at gaining more insight into the imaging properties of Cone Beam Computed Tomography (CBCT), in order to use it for patient position verification. For this purpose the On-Board Imager (OBI) by Varian Medical Systems has been simulated in order to study in particular the imaging of objects that are subject to respiratory motion, such as tumours in the thorax region.
Materials and methods: Series of individual CBCT projection images have been simulated, to be used for reconstruction into 3D images. These projections have been obtained by combining separate images of the primary and the scattered radiation. The image from the primary radiation has been calculated with analytical methods, while the one of the scattered component has been simulated with Monte Carlo methods, using the PENELOPE code system and the penEasy package. These have been normalized separately and added to form the combined image. For a phantom of cylindrical symmetry with a small moving tumour, the distribution of scattered radiation stays almost constant for all projection angles. Thus one image of the scatter distribution can be used for all projection angles, added to the images of primary radiation. This gives a considerable reduction in total calculation time. The projections of primary radiation, performed separately for each gantry angle, give information of the different tumour positions. In order to validate the simulations, the combined images have been compared with measured projection images, acquired with the OBI.
Results: Total simulated and measured images for different geometries agree well, generally within 3 %.

Multimodality & 4D image registration for IGRT: Opportunities and challenges

Marc L Kessler, PhD. Department of Radiation Oncology, The University of Michigan

Accurate target delineation and image guidance are essential components in precision radiotherapy. The definition of the GTV and various margins dictate the maximum radiation doses that may be safely delivered. Developments in multimodality and 4D imaging technologies are providing opportunities to improve tumour localisation and patient modelling for planning and to reduce setup variations and margins for delivery. Proper use of these technologies can provide greater sparing of dose to normal tissues and permit safer escalation of tumour doses. Techniques are also being developed to help predict response to treatment during therapy when interventions and adaptations are still possible. Optimal use of these technologies requires tools to spatially register the various image data, and once registered to integrate anatomical, functional and dosimetric information from the different imaging studies. Current planning and delivery systems do provide some form of these tools, though most support only simple geometrical models with limited degrees of freedom. Unfortunately, accurate registration of image data from clinical sites other than the brain or limited anatomical regions requires more degrees of freedom to properly model deformation, tissue sliding, and changes in tumour size and patient weight. The situation is further complicated by the realisation that the optimal number of degrees of freedom and other registration parameters vary from tissue to tissue. Using too few or too many degrees of freedom can cause inaccurate or non-physical results. Fortunately, development of sophisticated image registration algorithms which accommodate common anatomical and physiological processes is a very active area of research and promising techniques are emerging and undergoing clinical validation. This presentation will describe the current state of this technology and provide examples of the opportunities and challenges ahead.

Integration through registration: Deformable registration for IGRT

Kristy K Brock, Princess Margaret Hospital, University Health Network, University of Toronto

Image guided radiotherapy (IGRT) aligns the tumor identified at each treatment session to the location of the tumor identified during pre-treatment imaging and enables modification of the treatment plan to account for changes that occur over the course of treatment. The successful integration of these multi-modality images is often compromised by the soft tissue deformation that occurs between each acquisition. The use of deformable registration for the integration of multi-modality images for accurate tumor identification with volumetric images for IGRT will be discussed. Successful radiotherapy begins with an accurate identification of the tumor and normal tissue. The benefits of deformable registration for the integration of multi-modality images for tumor identification have been demonstrated for many sites, including liver and prostate. As advances are made in anatomical and functional imaging, the ability to accurate integrate these images into one model of the patient becomes increasingly important. The translation of the tumor, identified under ideal imaging settings through multi-modality images, must be translated onto the data obtained of the patient at the time of each treatment fraction. Rigid registration can successfully achieve this integration in many instances, however, anatomical sites which move due to physiological processes (e.g. respiration and bladder/rectal filling) often have more complex changes. In addition, tumors and normal tissues surrounding the tumor often respond over the course of radiation, changing in size and shape, as well as position. Examples of the benefit of deformable registration for IGRT and adaptation to anatomical changes will be presented for the head and neck, liver, and cervix.

Accelerating compute intensive image processing in image-guided radiotherapy

Karsten Østergaard Noe(a,d), Baudouin Denis de Senneville(d), Kari Tanderup(c), Thomas Sangild Sørensen(a,b). (a) Department of Computer Science and (b) Institute of Clinical Medicine, University of Aarhus, Denmark, (c) IMF, UMR 5231 CNRS / Université Bordeaux 2, France, (d) Department of Oncology, Aarhus University Hospital, Denmark

Introduction: For online IGRT, rapid image processing is needed. Fast parallel computations using Graphics Processing Units (GPUs) have recently been made more accessible through general purpose programming interfaces, We present a GPU implementation of the Horn and Schunck method for deformable registration of 4DCT lung acquisitions to exemplify the use of GPUs in IGRT.
Materials and methods: The registration is evaluated on the POPI-model acquired at the Léon Bérard Cancer Center, France. It consists of thorax CT image series (resolution 482×360×141 and voxel size 0.98×0.98×2.0 mm3) from 10 respiration phases in a free breathing volunteer and 41 anatomical landmark points in each image series. The registration method used is a multi-resolution GPU implementation of the 3D Horn and Schunck algorithm. It is based on the CUDA framework from Nvidia.
Results: On an Intel Core 2 CPU at 2.4GHz each registration took 30 minutes. On an Nvidia Geforce 8800GTX GPU in the same machine this registration took 37 seconds, making the GPU version 48.7 times faster. The nine image series of different respiration phases were registered to the same reference image (full inhale). Accuracy was evaluated on landmark distances before and after deformable registration. Original average landmark distance was 3.5 mm ± 2.0 mm (max = 14.0 mm). After registration, this average distance was equal to 1.1 mm ± 0.6 mm (max = 3.6 mm) which is well below the slice thickness of 2 mm.
Discussion: Using the GPU has led to a very significant reduction of the registration time due to the parallelized architecture of the GPU. Considering the slice spacing we find the registration result acceptable. The accuracy is comparable to previous results for the Demons algorithm in the POPI model (Vandemeulenboucke et al, ICCR 2007). The processing power of GPUs can be used for many image processing tasks in IGRT making it a useful and cost-effecient tool to help us towards online registration of images.

Characterisation of Radiotherapy Planning Volumes using Textural Analysis

William H. Nailon, Anthony T. Redpath and Duncan B. McLaren, Edinburgh Cancer Centre, Edinburgh, United Kingdom

Image processing techniques for automatic outlining are currently not able to contour to the accuracy required for radiotherapy applications. Image processing techniques based on statistical and fractal texture analysis were explored to determine their suitability for classifying the gross tumour volume (GTV), and other clinically relevant regions, on computerised tomography (CT) data. For eight bladder cancer patients, CT information was acquired at the radiotherapy planning stage and thereafter at regular intervals during treatment. Statistical and fractal features were calculated on the bladder, rectum and a control region on axial, sagittal and coronal CT image data. The results demonstrate the significant sensitivity of using a reduced feature set for characterising the pathology of the GTV and the potential that the approach has for development towards a computer-assisted outlining tool for radiotherapy applications.

An investigation of the accuracy of radiotherapy dose plans calculated on the basis of tissue-segmented CT images

Eilertsen K, Nilsen L, Vestad T A, Geier O, Skretting A. Department of medical physics, The Norwegian Radium Hospital, Oslo, Norway

Introduction: The advantage of MRI-based radiotherapy planning is the superior soft tissue differentiation. However, for accurate patient dose calculations, a conversion of the MR images into Hounsfield CT maps is necessary. The aim of the present study was to investigate the dose accuracy that can be achieved using CT planning images where the density of bone and soft tissue was manipulated. This study will serve as a reference for the dose accuracy obtained when using MR images in dose calculations.
Material and methods: Treatment plans for ten prostate cancer patients were selected. The collapsed cone algorithm (Masterplan, Nucletron BV, The Netherlands) was used to calculate patient dose distributions. The dose calculations were based on four different image sets: CT(DP): Original CT-series CT(W): Soft tissue and bone density set to 1.02g/cm3 CT(W+B1.3): As above, but bone density 1.3g/cm3 CT(W+B2.1): As above, but bone density 2.1g/cm3 The dose distributions were compared by analysing dose difference histograms as well as through a visual display of spatial dose deviations.
Results: The population based minimum, mean and maximum dose difference between CT(DP) and CT(W) in the target volume was -2.8, -1.0 and 0.6 %, respectively. Corresponding differences between CT(DP) and CT(W+B1.3) were -1.6, 0.2 and 1.5 %, respectively, and between CT(DP) and CT(W+B2.1) -4.3, 4.2 and 9.7 %, respectively. For the rectum, the differences between CT(DP) and the other image sets were in the range of -19.5 to 8.8 %. For the bladder, the differences were in the range of -9.6 to 7.0 %.
Discussion: The difficulties associated with the segmentation of bone in MR images were not addressed in the current work. Instead, a systematic study using CT images was undertaken, which showed significant dose deviations between the original and manipulated planning basis. When real MR images is introduced, errors in tissue segmentation and errors that stem from geometrical non-linearities may further reduce the dose calculation accuracy.

A phantom for characterization of geometrical linearity in MR

Vestad TA, Geier OM, Eilertsen K, Skretting A. Department of Medical Physics, the Norwegian Radium Hospital, Rikshospitalet HF, Oslo, Norway

Introduction: As part of the quality assurance of the ongoing implementation of MR in radiotherapy treatment planning at the Norwegian Radium Hospital, a novel phantom for characterization of geometrical linearity has been designed, built, and tested.
Materials and methods: The phantom consists of a Perspex box with an inner volume of 440x320x300 mm3. Silicone cords (2.0 mm in diameter) are spanned horizontally in the z-direction of the phantom between holes in opposite walls that form an equi-distant grid of rows and columns in the x,y-plane. These allow for identification of the x- and y-components of the geometrical image distortions. Skewed cords, at a steep angle to the x-axis, are included for quantification of deviations in plane position (slice curving), since such deviations lead to x-shifts of the intersection point. The phantom was intentionally constructed in such a way that image series can be automatically analyzed by an in house written IDL (ITT) computer program to derive the positional deviations from linearity in axial planes as well as deviations in plane positions. When used, the phantom was immersed in a water tank and its position adjusted so that the z-direction coincided with the direction of the B0-field. Silicone cords in water provide adequate contrast in MR images for most pulse sequences. The phantom was scanned on the Siemens MAGNETOM Espree 1.5T. In the experiment reported here, a 3D turbo spin echo sequence (SPACE) was used. The MR images (288 images, FoV 450x450 mm2, voxel size 1x1x1 mm3) were post-processed using the gradient distortion correction algorithm (3D) provided by the vendor.
Results: The inherent geometrical linearity presented by our MR is poor and inadequate for use in radiotherapy treatment planning. However, the images of x,y-planes obtained by application of the (3D) distortion correction algorithm provided by the vendor demonstrate significant improvements. The computer program identified all the cords in the image of the isocentre plane and was able to track most of them through the other images and thus compute deviations at different z-positions.
Discussion: Our method allows for rapid quantification of system-induced geometrical image distortion for all relevant positions in the MR scanner.

Physics aspects of prostate tomotherapy: Planning optimization and image-guidance issues

C. Fiorino[a], C. Cozzarini[b] , S. Broggi[a], G.M. Cattaneo[a], F. Alongi[b], N. Di Muzio[b], P. Mangili[a], L. Perna[a], F. Fazio[b], c, R. Calandrino[a] [a]Medical Physics, S. Raffaele Institute, Milano, Italy, [b]Radiotherapy, S. Raffaele Institute, Milano, Italy, [c]IBFM CNR, Milano, Italy.

Purpose: To review planning and image-guidance aspects of more than 3 years experience in the treatment of prostate cancer patients with Helical Tomotherapy (HT).
Methods and materials: Planning optimization issues concerning two Phase I-II clinical studies were addressed: in the first one, 58 Gy in 20 fractions were delivered to the prostatic bed for post-prostatectomy patients: in the second one, a simultaneous integrated boost (SIB) approach was applied, with prostate dose equal to 71.4 Gy or 74.2 Gy in 28 fractions, depending on the risk class, concomitantly delivering 65.5 Gy to the overlap between PTV and rectum. On-line daily image guidance using the MVCT system integrated in the HT unit was applied. Bone match was used for post-operative patients while prostate match was applied for radically treated patients. MVCT data of a large sample of both categories of patients were recently reviewed.
Results: At now, more than 250 patients were treated. Planning data show the ability of HT in creating highly homogeneous dose distributions within PTVs. Organs at risk (OAR) sparing also showed to be excellent. In a recent planning study comparing HT and inverse-planned IMAT, HT compared favourably in terms of coverage and homogeneity of the dose distribution while keeping similar OAR sparing, excepting for the penile bulbus where, although the prescribed constraints were satisfied, HT was detrimental. In the case of pelvic nodes irradiation, a large sparing of bowel was evident compared to 3DCRT and conventional 5-fields IMRT. The analysis of prostate motion data relative to bony anatomy showed a limited motion of the prostate (about 5 % of the fractions show a deviation ³ 3 mm), due to the careful application of rectal emptying procedures. Based on phantom measurements and on the comparison with intraprostatic calcification based shift assessment, direct visualization prostate match seems to be sufficiently reliable in assessing shifts greater or equal to 3 mm.
Conclusions: HT offers excellent planning solutions for prostate cancer, showing to be highly efficient in a SIB scenario. Daily MVCT information showed evidence of a limited motion of the prostate in the context of rectal filling control easily obtained by instructing patients in self-administrating a rectal enema.

IGRT in rectal cancer

Vincenzo Valentini, Radiotherapy Department, Università Cattolica S.Cuore, Rome, Italy

To date, no great interest has been shown in clinical implementation of recent IGRT modalities in rectal cancer since only few studies have been published on this issue. This may partially be explained by the fact that with current treatment modalities locoregional recurrences are already very low (around 10%). However, there is still room for improvement in treatment of high risk patients (T3-4, N+). In these patients we may achieve better results by improving our radiation treatment technique from simple 2D to 3D. But before introducing IMRT for rectal cancer in order to spare small bowel, we need a proper definition of our CTV and PTV.
The clinical target volume should encompass the tumour site, the entire mesorectum with its fascia and the lateral nodes, widely recognized as the most likely sites of local recurrence, with different incidence according to tumour stage at diagnosis. 2D planning based on bony anatomy showed to be less reliable than 3D irradiation in terms of patterns of dose distribution and target coverage.
Recent studies discussed the correct delineation of these target volumes and the appropriate PTV margin recipes in order to manage set-up errors and organ motion. In an observational study carried out in Leuven University in collaboration with our institution several variations in mesorectum shape were observed.
A systematic review on rectal organ motion together with the data from our experience led to the awareness that an appropriate control of target location and changes in tumour and mesorectum during treatment is necessary. Image-guided radiation therapy, could help us to follow the target volume and organs at risk during the course of treatment, allowing adjustments to improve accuracy in dose delivery, especially when dose escalation studies are planned in the treatment of rectal cancer.

Image guided adaptive brachytherapy in cervix cancer

Richard Pötter, Medical University of Vienna, General Hospital Vienna, Austria

A new paradigm for an image guided treatment (planning) chain has recently been introduced for cervix cancer brachytherapy going from clinical and MRI based tumour assessment at diagnosis through multiple steps to final 3D assessment of disease control and treatment failure, respectively (including morbidity evaluation).
This paradigm includes more general issues specific for brachytherapy which cannot be specifically addressed during this lecture as provisional image based planning, imaged guided applications and definitive image based treatment planning („Imaging" in: GEC ESTRO Handbook of BT 2002) as well as the concept of adaptive treatment planning taking into account tumour shrinkage and change of topography during external beam radiochemotherapy and at each fraction of brachytherapy,
Specific issues of major importance for this approach are the concept of adaptive target definition (High Risk (HR) and Intermediate Risk CTV) (Haie-Meder et al. R&O 2005) and the contouring of Organs at Risk (OAR) for each fraction. Furthermore appropriate imaging of the applicator in situ indicating the possible source positions together with the GTV, the cervix, the uterus, and adjacent OAR needs particular attention (Hellebust et al. PhysMedBiol 2007). Accurate image based reconstruction of the applicator is essential, in particular for limiting systematic uncertainties in dose calculation (Tanderup et al., R&O 2008, in press).
For treatment planning specific dose volume parameters have been introduced (Pötter et al. R&O 2006), that will be reviewed during this presentation taking into account their clinical validity as evaluated from the Vienna series in 141 patients and from some limited experience reported in literature.
D90 for the HR CTV seems to be an appropriate tool for evaluating target coverage as interobserver variation is mall (conformitiy index 0.8) and the predictive value for outcome is high. Above a minimum dose to the 90% of the HR CTV of 87 Gy (EQD2) the risk of local recurrence was 4% compared to 20% for lower doses (Dimopoulos et al. IJROBP submitted).
The cumulative dose in 2 ccm of the rectum has a high correlation to the ICRU rectum point. Morbidity seems to be low (G3 and G4 <5%), if the dose is kept below 75 Gy EQD2 (Koom et al. IJROBP 2007; P. Georg et al. R&O submitted).
The cumulative dose in 2 ccm of the sigmoid is not well correlated with a clinical or endoscopic endpoint. Reasons for these findings may be uncertainties due to sigmoid movements from fraction to fraction (Sturzda et al. Brachyhterapy 2008 (abstract)).
The cumulative dose in 2 ccm of the bladder has poor correlation to the ICRU bladder point and also poor correlation to clinical outcome. Reasons fort his may be different bladder filling and/or little correlation of morphologic changes to functional outcome for different locations of the high dose region, e.g. in the posterior bladder wall or in the bladder neck.
For the assessment of vaginal morbidity no clear dose volume concept could be established yet, due to uncertainties in dose calculation (sharp dose fall-off) and contouring (mm) (Berger et al. IJROBP 2007). For clinical outcome assessment, it has to be taken into account, that the upper vagina adjacent to the cervix is located in the very high dose region (>>100 Gy) where the plateau of the dose effect curve may have been reached.
A multicentre international clinical study on MRI based brachytherapy in cervix cancer (EMBRACE) has just been started aiming at 600 patients within three years.

Image-guidance protocol comparison: supine and prone setup accuracy for pelvic radiation therapy

F. Siddiqui[1], C. Shi[2], N. Papanikolaou[2], M. Fuss[1] [1]Oregon Health & Science University, Portland, OR, USA, [2]The University of Texas Health Science Center at San Antonio, San Antonio, TX, USA

Purpose: To investigate the impact of different image-guidance protocols, and patient setup on residual setup error for radiation therapy of pelvic malignancies. We aim to identify an optimal frequency and protocol for image-guidance.
Materials: Using daily online image-guidance data from 30 patients (829 MVCT; 299 prone setup on belly board, 530 supine setup), we retrospectively assessed the impact of various image-guidance protocols on residual setup error.
Results: Of 5 protocols analyzed, daily imaging with a running mean for day to day offline setup correction provided best setup error reduction. A daily running mean protocol would have reduced the average length of 3D vector shifts for setup optimization from 15.6, and 12.9 mm for prone and supine setup, to 5 mm and 5.4 mm, respectively. A No Action Level (NAL) protocol, averaging shifts of the first 3 fractions, would have reduced the respective setup variability to 6.3 mm (prone) and 7.5 mm (supine). An extended NAL (eNAL) protocol, averaging shifts of the first 3 fractions plus weekly imaging, would have reduced the daily positioning variability to 6 mm for both prone and supine setups. Daily image-guidance without change in patient setup resulted in setup corrections >10 mm in 64.3% for prone and 70.3% for supine position. Using the NAL protocol reduced the respective frequency to 14.4%, and 21.2% for prone, and supine positioning. In comparison, using a daily running mean protocol reduced shifts >10 mm to 5.5% (prone), and 8.3% (supine), respectively.
Discussion: While daily online image-guidance is considered the gold standard for this analysis, the least positional variation or shift was observed with daily imaging and running mean setup correction for subsequent treatment days. However, both NAL, and eNAL protocols provide comparable vector variation control with significantly lower frequency of imaging. While the mean 3D vector of corrective shifts was greater for prone setup compared to the supine setup, using any image-guidance protocol would have reduced shifts for prone setup to a greater extent than for the supine setup. This indicates a greater risk for systematic errors in supine setup. Other protocols, such as weekly imaging (every 5th fraction) and averaging shifts for the first 5 fractions did not yield better results than the NAL or the eNAL protocol.

Intra-fractional prostate motion and set-up error progression studied by continuous electronic portal imaging

Torbjørn Månsson Haskå, M.Sc.[a], Henriette Honoré, Ph.D.[a], Ludvig Paul Muren, Ph.D.[a,b], Morten Høyer, Ph.D.[b] and Per Rugaard Poulsen, Ph.D.[a,b,c] [a]Aarhus University Hospital, Department of Medical Physics, Denmark. [b]Aarhus University Hospital, Department of Oncology, Denmark. [c]Stanford University, Department of Radiation Oncology, USA.

Purpose: The use of marker-based on-line image guided radiotherapy for prostate cancer has considerably reduced the treatment margins to sub-cm. In this study we have quantified the residual set-up errors remaining after isocenter correction, studied their development during beam delivery and estimated their impact on margins.
Methods and Materials: After initial on-line patient set-up based on orthogonal kV x-ray images of implanted fiducial markers, continuous electronic portal imaging was performed during treatment delivery in 10 out of 39 treatment sessions for 20 prostate cancer patients. The cranio-caudal (CC) position of the centre-of-mass of the three markers was found using a threshold technique on every single image frame for all patients, typically 12-14 images for 5 treatment beams in every fraction. The CC prostate position was determined relative to its initial position at treatment onset and relative to its planned position within the field aperture. These results allowed determination of the CC intrafraction prostate motion and the CC intrafraction set-up error progression, respectively.
Results: At treatment onset the standard deviation (SD) of the set-up error was 1.0 mm in the lateral direction and 1.5 mm in the cranio-caudal (CC) direction. It did not depend significantly on the duration of the set-up procedure (mean: 3.0 min, span 1.2 – 14.6 min). The distribution of CC prostate positions relative the position at treatment onset broadened from 0 mm to 1.4 mm during the treatment session, while the corresponding CC setup error distribution broadened from 1.5 mm to 1.9 mm. This broadening means that the necessary CC setup margin increased by around 1 mm during the treatment fraction.
Conclusions: Large differences in the intrafraction CC prostate motion patterns were found, however, intrafraction motion only results in a modest additional CC set-up margin of around 1 mm relative to the margins needed for the residual set-up error at treatment start.

A new fiducial marker for image-guided radiotherapy of prostate cancer

Jesper Carl, Jane Nielsen, Martin Skovmos Nielsen, Mats Holmberg, Erik Højkjær Larsen, Knud Fabrin, Rune V. Fisker, Dept of Medical Physics, Aalborg Hospital, Aalborg, Denmark.

Use of doses beyond 80 Gy in External Beam Radio Therapy (EBRT) of patients with prostate cancer requires that irradiated volume of normal tissue is minimized in order to avoid unacceptable side effects. This implies good accuracy of delineation of Clinical Target Volume (CTV) and accurate positioning of CTV in each EBRT session. To accomplish these goals a new fiducial marker for image guided radiotherapy (IGRT) is under development. This new marker is based on a removable Ni-Ti prostate stent as an alternative to implantable gold markers and other methods. The new marker has been developed during two previous clinical feasibility studies. The marker is currently being used for IGRT treatment in a third clinical study. The new marker is visible on both X-ray and MR with good contrast. Consequently the marker is used to co-register MR and planning CT scans with high accuracy in the region around the prostate. The co-registered MR-CT is used for delineation of GTV before planning. After planning the CT images and treatment plan isocenter are transferred to the IGRT system, Exactrac® Robotics from Brainlab. In each treatment session the IGRT system is used to position the patient before treatment. The IGRT system use a stereo pair of kV images matched to corresponding Digital Reconstructed Radiograms (DRR) from the planning CT scan. The match is done using mutual gray scale information. The pair of DRR's for positioning is created in the IGRT system with a threshold in the Look Up Table (LUT). This leaves only high density objects, as the new marker, to show up in gray scale values. The IGRT system is then able to perform an automated match of kV images to DRR's using the stent. The resulting match provides the necessary shift in couch coordinates, including pitch and roll angles of the couch table top, to position the stent with an accuracy of 1-2 mm within the planned position. As the stent is also clearly visible on images taken with high voltage x-rays using electronic portal images devices (EPID) the position can be verified independently of the IGRT system. A detailed description of the method will be given. Data on the approximately 30 patients that has been treated up to this point in time with this new technique together with clinical experience of the IGRT system will also be presented.

A comparison between skin, bone and gold markers for prostate external radiotherapy treatment: Impact on PTV margins

Kylling, A., Jensen, C., Resell, M. and Skottner, N., Department of Oncology, Ålesund Hospital, Ålesund, Norway

For external beam radiotherapy of the prostate, fiducial markers are used for positioning of the patient. Positioning using skin markers, bony anatomy or gold seeds give potentially different levels of uncertainty in treatment delivery. For prostate patients without implanted gold seeds, cone-beam CT (CBCT) scans have been performed at regular intervals during treatment. Three-dimensional comparison of the CBCT scans with the dose planning CT scan is made. Thus comparing positioning using skin markers with the bony anatomy. From these comparisons standard deviation of preparation (systematic) errors and execution (random) errors are calculated. Utilizing the margin recipe of van Herk et al (2000) PTV margins pertinent to the clinic are calculated. For prostate patients with implanted gold seeds, comparisons are made between the bone anatomy and the gold seeds to detect motion of the prostate with respect to the bone anatomy. From the comparison of CBCT scans and the dose planning CT scan, PTV margins of 5mm (LR), 5mm (CC) and 7mm (AP) are calculated. These PTV margins are applicable when using skin markers. Preliminary results for the implanted gold seeds indicate that the apex of the prostate moves on the order of a few mm compared to the bony anatomy. However, for some patients the filling of the rectum may cause large rotations around the LR axis. The margins calculated with the van Herk et al (2000) margin recipe do not include rotations and are thus minimal margins. Currently, the clincal used PTV margin is 15mm in all directions, except in the dorsal direction where 10mm is used. The above results suggest that these margins may be somewhat reduced. The use of gold seeds increases treatment delivery accuracy and potentially allows a further shrinking of margins.

The impact of on-line correction for rotational organ motion in image-guided radiotherapy of the bladder and prostate

Redpath AT(1), Wright P(2) and Muren LP(2), (1) Dept of Oncology Physics, Western General Hospital, Edinburgh, Scotland; (2) Dept of Medical Physics and Dept of Oncology, Aarhus University Hospital, Aarhus, Denmark

Introduction: Current basic IGRT methods only correct for translation of organ position through a 3D movement of the treatment couch. The aim of this study was to quantify the relative importance of rotational vs. translational corrections in IGRT for pelvic targets (focusing on treatment of bladder and prostate alone).
Materials and methods: The data material consisted of a set of 9 bladder cancer patients (6 male, 3 female) each having a planning CT scan and between 3 and 8 repeat CT scans throughout their treatment course. The bladder and prostate were outlined on all scans, making a total of 62 repeat bladder and 44 repeat prostate CTVs available. An algorithm was written to determine both the optimum 3D translation and the rotation angles required in order to align the repeat CTVs with their planning CTV. Angles considered were those possible through gantry rotation, couch rotation and couch tilt. The optimum shifts and angles were determined as those that will minimise the volume of the repeat scan CTV lying outside the volume of the planning CTV. Three different situations were investigated: 1) 3D translation only (3 DoF), 2) rotation after applying the optimum 3D translation (3+3 DoF) and 3) translation and rotation optimised concurrently (6 DoF).
Results: For the bladder, the overall average volume percentage (across scans and patients) of the repeat CTV not included in the planning scan CTV was reduced from 13.2% without IGRT to 9.4%, 9.1% and 8.9% with 3DoF, 3+3 DoF and 6 DoF, respectively. For 12 of the 62 repeat bladder CTVs, a reduction greater than 5% in the volume not covered was obtained when including rotation. For the prostate, the overall average of the repeat CTV not enclosed by the planning CTV was reduced from 25.5% without IGRT to 16.3%, 16.2% and 16.1% with 3DoF, 3+3 DoF and 6 DoF, respectively. The largest reduction obtained using 6 DoF in stead of 3 DoF for the prostate was 3%.
Conclusion: When treating either the bladder or prostate alone, translational IGRT correction was by far the most important action necessary to ensure alignment of the repeat CTV with the planning CTV. As it is the largest positional deviations that determine the margins required, further investigation of the impact in terms of margins are currently being performed.

Optimal treatment margins for complication-free curative radiotherapy based on interfraction tumor displacement and organ deformation

Arnesen MR, Eilertsen K, Malinen E. Department of Medical Physics, Division of Cancer Medicine and Radiotherapy, Rikshospitalet University Hospital, Oslo, Norway

Purpose: To present a methodology to estimate optimal treatment margins for complication-free curative radiotherapy based on interfraction tumor displacement and organ deformation.
Materials and methods: Cone beam CT images of a prostate cancer patient undergoing fractionated radiotherapy were acquired at all treatment sessions. The clinical target volume (CTV) and organs at risk (OARs; bladder and rectum) were delineated in the images, generating a library of 3D CTV-OAR configurations. Random sampling from the library was performed in order to simulate fractionated radiotherapy including intra- and interpatient variability in setup and organ motion/deformation. For each simulated patient, four treatment fields defined by multileaf collimators were automatically generated around the planning CTV. The treatment margin, defined as the distance from the CTV to the field border, was varied between 2.5 and 20 mm. Resulting dose distributions were calculated by a convolution method. Doses to OARs (experiencing interfraction deformations) were estimated by polynomial warping, while the CTV (experiencing interfraction displacement) was assumed to be a rigid body. The equivalent uniform dose (EUD), the tumor control probability (TCP) and the normal tissue complication probability (NTCP) were used to estimate the clinical effect.
Results: The simulations produced population based EUD histograms for the CTV and the OARs. The number of patients receiving an optimal target EUD increased with increasing margins, but at the cost of an increasing number receiving a high EUD to the OARs. Calculations of the probability of complication-free tumor cure and subsequent analysis gave an optimal treatment margin of about 10 mm for the simulated population.
Conclusions: The current work illustrates the principle of optimal treatment margins based on both tumor and normal tissue characteristics. Clinically applicable margins may be obtained if a large patient image database is available.

The normal tissue sparing potential of adaptive strategies in radiotherapy of bladder cancer based on fiducials

P Wright[a], AT Redpath[b], J Søndergaard[a], M Høyer[a], C Grau[a], LP Muren[a]. [a]Dept of Oncology and Department of Medical Physics, Aarhus University Hospital, Aarhus C, Denmark [b]Dept of Oncology Physics, Western General Hospital, Edinburgh, Scotland

Introduction: To improve the outcome in bladder RT we have investigated various adaptive treatment strategies involving on-board tumour/target visualisation using fiducials. The strategies are compared in terms of the amount of normal tissue enclosed within the PTV.
Materials and methods: CT data of five male bladder cancer patients having a planning and 7-8 repeat scans during treatment were used for this study. Various tumour positions (at the sup/inf/ant/post/left/right wall) were identified in the repeat scans based on a reference co-ordinate system. The origin of this system was positioned half-way between the centre of mass of the bladder and the entrance point into the bladder along an axis through the centres of masses of the prostate and the bladder. The repeat CTVs were translated, so that the tumour positions overlapped with the corresponding position on the planning CTV, whereafter the required margins were determined using a previously published margin calculation algorithm (Redpath and Muren, Radiother Oncol 2005; 77: 194-201). These calculations were performed both to find the margins required to enclose all repeat scans at the same time (standard PTV) and those to enclose the repeat scans one by one, i.e. simulating adaption on daily basis (adaptive PTV). Results were compared both with the case of optimising the margins for all repeat scans first without any shift of the contour (no image-guidance) and second after finding the best shift for the whole bladder in order to minimise the PTV volume (whole-bladder shift).
Results: The volume of normal tissue enclosed within the PTV for the inferior and superior position's standard PTVs was not notably different from the case of no image-guidance (197, 226 respectively 208 cc). The standard PTV for the superior position gave the largest normal tissue volume. When covering all repeat scans the strategy of optimal shift is superior (excess volume 168 cc). Anyway, the adaptive PTV strategy is most favourable in terms of normal tissue sparing. Compared to the standard PTV, the adaptive PTV nearly halved the volume of normal tissue included.
Conclusion: By daily adaptation of the treatment the normal tissue irradiation could be considerably reduced. Further, this could open for dose escalating the tumour without increasing the side effects.

A dose planning study on applicator guided stereotactic IMRT boost in combination with 3D MRI based brachytherapy in locally advanced cervical cancer

Marianne S Assenholt, M.Sc.[1], Jørgen Petersen, M.Sc.[1], Søren K Nielsen, PhD.[1], Jacob C Lindegaard, D.M.Sc.[2] and Kari Tanderup, PhD.[1,2]. [1]Dept. of Medical Physics, Aarhus University Hospital, 8000 Aarhus, Denmark, [2]Dept. of Oncology, Aarhus University Hospital, 8000 Aarhus, Denmark

Purpose: Locally advanced cervical cancer is usually treated with external beam radiotherapy and intracavitary (IC) brachytherapy (BT). In case of poor response it may be difficult to reach a sufficient BT dose. The purpose of this study was to explore whether an applicator guided stereotactic IMRT boost could be used to improve tumour coverage.
Methods: Dose plans of 5 patients with tumour volume of 31-100cc at the time of BT were analysed. MRI was performed with a combined intracavitary/interstitial (IC/IS) ring applicator in situ. A radiotherapy schedule consisting of 45Gy (1.8Gy x 25) IMRT (tumour and elective target) followed by 4 boost fractions of 7Gy was modelled. Dose prescription to the HR-CTV was 84Gy (EQD2). Four different boost techniques were evaluated: IC-BT, IC/IS-BT, IC-BT+IMRT and IMRT. All dose plans were optimised for maximal tumour dose and coverage while respecting DVH constraints in organs at risk: D2cc < 75Gy in rectum and sigmoid and < 90Gy in bladder (EQD2). In combined BT+IMRT dose plans, the IMRT plan was optimised on top of the BT dose distribution. A 3mm PTV margin was used in IMRT. In IMRT alone the central part of the target was escalated to 110Gy (EQD2) to mimic dose inhomogeneity in BT. V60Gy (EQD2) was evaluated outside HR-CTV. In combined BT+IMRT the dose plan robustness to setup uncertainties was evaluated by displacing the IMRT dose distribution by +/- 3mm in the direction of the most steep dose gradient.
Results: Median dose coverage in IC plans was 73% [66-91%]. By using IC/IS or IC-BT+IMRT boost, the median coverage was improved to 93% [78-97%], and to 97% [69-99%] respectively. For IMRT alone, a median coverage of 93% [90-100%] was achieved, but V60Gy volumes outside HR-CTV were significantly increased by a mean factor of 2.2 [1.5-2.6] compared with IC/IS. It depended on individual tumour topography whether IC/IS-BT or IC-BT+IMRT boost was the most favourable technique. Setup errors of 3mm will not result in hot or cold spots in the junction region in combined BT+IMRT plans.
Conclusion: In this study the dose coverage could be significantly increased by adding IC-BT or IMRT boost to intracavitary dose. Sufficient target coverage could be obtained by IMRT alone, but the V60Gy (EQD2) was significantly increased. It is technically possible to create robust dose plans that combines image guided BT and IMRT.

The role of image guidance in respiratory gated radiotherapy

Stine Korreman, Trine Juhler-Nøttrup, Gitte Persson, Marika Enmark, Anders Pedersen and Lena Specht, Department of Radiation Oncology, Rigshospitalet, Copenhagen University Hospital

Respiratory gating for radiotherapy beam delivery is a widely available technique, manufactured and sold by most of the major radiotherapy machine vendors. Respiratory gated beam delivery is intended to limit the irradiation of tumours moving with respiration to selected parts of the respiratory cycle, and thereby enable reduction of the required treatment field margins.
Without adequate use of respiratory correlated image guidance on a regular basis, respiratory beam gating may however have a detrimental effect on target coverage. Image guidance of tumour respiratory motion is therefore of utmost importance for the safe introduction of respiratory gating.
In this presentation, suitable image guidance strategies for respiratory gated radiotherapy are reviewed for three cancer sites; breast cancer, lung tumours and liver tumours.

Active breath control and in-vivo portal dosimetry for lung tumours

A. Piermattei[1,3], S. Cilla[1], L. Grimaldi[1], B.G. Augelli[1], G. D'Onofrio[1], F. Deodato[2], C. Digesù[2], A. Fidanzio[3], A.G. Morganti[2] [1]U.O. Fisica Sanitaria, Università Cattolica S. Cuore (Campobasso),[2]U.O. Radioterapia, Università Cattolica S. Cuore (Campobasso),[3]Istituto di Fisica, Università Cattolica S. Cuore (Roma)

Introduction: For targets in thoracic and abdomen region, the organ motion due to breathing limits the precision of Radiotherapy. Field sizes must be sufficiently large to take into account tumour motion and this means a limitation in the dose that can be safely delivered. Active breathing control (ABC) techniques can supply a good immobilization of respiration motion by monitoring the patient's breathing cycle. However, variations of the target position cannot be completely reduced and an in-vivo dosimetry method was applied to verify the correct dose delivery.
Material and methods: Five patients with lung tumours were treated using the Elekta ABC device. This device was used to irradiate the target at the end of the inhale phase. The breathing cycle is plotted on a remote computer that shows the graphic readout of the tidal volume (in dm3) over time. The patients are educated in ABC practice sessions for CT data acquisition and irradiation. The electronic portal images (EPI) for every fraction therapy were analyzed and an in-vivo dosimetry at the isocenter point (adopted by the authors in other experiences) based on signals from EPID was applied.
Results: Correlations between the daily tumour shifts (by EPI) and the breath-hold volume (BHV) were observed. Moreover, the in-vivo dosimetry method, that is characterized by a tolerance action level of 5%, confirmed the need to irradiate the patient in a reproducible breath-hold, that means with a reproducible breath-hold volume. For patients that presented changes in size, location and shape of tumour, the in-vivo dosimetry supplied a tempestive warning to acquire new CT scans during the treatment for eventual adaptive radiotherapy.
Conclusion: The intra-fraction and the inter-fraction reproducibilities by ABC of lung tumour position present variations up to 4 mm (1 SD). Moreover the tumour position reproducibility changes with the BHV. For these reasons we have examined the possibility to treat lung tumours with the ABC device analyzing (i) the EPI in every fraction of treatment, (ii) the BHV values and (iii) the dose at the isocenter point. These controls supply a useful information to proceed with new CT scans for eventual adaptive radiotherapy.

Lung and heart dose volume and function study of image guided respiratory gating radiotherapy for left breast cancer treatment using deformable imaging registration

Zhang S, Castillo R, Woodward W, Guerrero T, Buchholz T. University of Texas MD Anderson Cancer Center

Purpose: To evaluate the heart and lung sparing with deep inspiration breath-hold (DIBH) respiratory gating radiotherapy for left breast cancer.
Method and Materials: Patients were selected for breath-hold (BH) gating study after heart protrusion into the treatment field during the free-breath (FB) CT scan. The Varian Real-time Position Management (RPM) system was used to monitor the patient respiratory motion during the deep inspiration breath-hold (BH) CT scan. Both the FB and BH CT dataset were co-registered into the Philips Pinnacle treatment planning system. The treatment plans were optimized with tangent fields using field-in-filed technique. The Varian linear accelerator coupled with RPM system was used for gating treatment. The On-Board-Imaging (OBI) system was used to assure the same lung volume at the different cycles of BH in the gating treatment as in the BH CT simulation. For dosimetric comparison the treatment beam and MLC parameters generated for the BH treatment were transferred to the plan with FB CT dataset. The lung dose volume was imported to an in-house developed deformable imaging registration algorithm for function study.
Results: Breath-hold was well accepted by the patients, with treatment duration for each field typically less than 15 seconds. The total lung volume was significantly increased due to deep inspiration, up to 2 times volume as in the normal free-breath. However the BH lung volume in the treatment fields was comparable to the FB lung volume. The relative lung volume received more than 50% of the prescribed target dose was reduced to the order of 10 -20%. For all patients DIBH moved the heart completely out of the radiation fields. The heart volume received more than 10 Gy dose was reduced from 5-10% in the FB to less than 1% in the BH gating treatment.
Conclusions: Remarkable potential is shown for DIBH gating radiotherapy to reduce the risk of both cardiac mortality and pneumonitis for the left breast irradiation.

Can respiratory coaching for 4D CT emulate free breathing during the treatment course?

Persson GF, Nygaard DE, Olsen M, Pedersen AN, Specht L and Korreman SS. Dept. of Radiation Oncology, Rigshospitalet, Copenhagen, Denmark

Introduction: Using 4D CT and finding the midventilation scan for planning in lung cancer radiotherapy diminishes the risk of introducing a systematic error caused by tumor motion. The image quality of 4D CT depends on breathing regularity. Respiratory coaching may improve regularity, facilitating less motion artifacts. We question the safety of coached planning 4D CT without coaching during treatment. For this purpose we investigated whether it is possible to coach to a more regular breathing close to the free breathing.
Methods: 11 volunteers, recruited among health professionals in the department, went through auditive respiratory coaching on 3 different days within a 2 week period. The RPM system (Varian) was used to track the respiratory motion. On all days, free breathing and two coaching modes were recorded. All breathing curves are being analyzed regarding amplitude to find inter- and intrasession variations. We assumed that first day's free breathing simulated an uncoached 4D CT planning and compared the mean amplitude to the mean amplitudes of the free and coached breathing from day 2 and 3. We equally assumed that the coached breathing from day1 simulated a coached 4D CT planning and compared the mean amplitude to the mean amplitudes from the free and coached breathing from day 2 and 3 (two tailed T-test, $p<0.05$).
Results: Comparing the first day's free breathing with free breathing the following days revealed a significant increase in amplitude for 7 volunteers and a significant decrease for 2. Comparing the first day's coached breathing to free breathing the following days showed an increase in amplitude for half the volunteers and a significant decrease for 2. Comparing first day's coached breathing to the coached breathing the following days showed a significant increase in amplitude for 9 volunteers and a significant decrease for 2.
Discussion: These preliminary results suggest that large interfraction variation is present in breathing amplitude irrespective of coaching. This suggests that daily image guidance should be applied to verify respiratory pattern and tumor related motion. Fluoroscopy study investigating the effect of coaching on the interfraction tumor motion is warranted. Until further investigated it is not recommendable to use coached 4DCT for planning of a free breathing treatment course.

4DCT image-guidance for SBRT

M. Fuss[1], A. Srisuthep[2], J. Kalpathy-Cramer[3], W. D'Souza[1]
[1]Radiation Medicine, and [3]Medical Informatics and Clinical Epidemiology, Oregon Health & Science University, Portland, OR, USA, [2]Radiation Oncology, Bhumibol Adulyadej Hospital, Bangkok Thailand

Purpose: To investigate changes in target volume, respiration target motion trajectory and motion envelope over 3 to 5 fraction SBRT for lung cancer.
Materials: Fifteen patients underwent 4DCT simulation, and repeat 4DCT imaging for SBRT image-guidance (59 re-4DCT; 1-5 re-4DCT/patient, median 5). Target volumes were individually delineated in the following CT data sets: free-breathing (FB), 10 respiratory phases (0-90%), MIP, MinIP, and AveIP. We analyzed target volumes, and assessed if typical SBRT PTVs (PTV-FB: GTV-FB + 5 mm axial, 10 mm craniocaudal; PTVMIP: ITV-MIP + 5 mm) would encompass the motion envelop during the SBRT course.
Results: In this sample, target volumes were stable (+/- 10%) over a course of SBRT in 11 patients; 2 tumors did shrink by up to 39%, while 2 tumors increased in size by up to 36%. Shape of the motion trajectory was characteristic for individual patients over the SBRT course in 13/15 patients, while maximum respiration target centroid displacement was more variable. Inter-individually, motion trajectory shapes varied widely. The respective motion envelope coverage by the clinically utilized PTV-MIP was better than 90%. While the PTV-FB provided similar coverage, the respective volumes differed from PTVMIP by up to 20 % (mean 114%).
Discussion: In this preliminary analysis, 4DCT based image-guidance assessed changes in target motion over time were observed in over 50% of patients. Individually, significant changes in respiratory target motion were observed that prompted adaptive re-planning to minimize the risk of target miss (n=2) or allowed for significant normal tissue sparing (n=1). Changes in target motion were randomly observed early and late in the SBRT course, and were individually not predictive of motion during the following fraction.

On-line image guidance for stereotactic radiotherapy of lung malignancies by cone beam CT: comparison between target localization and alignment on bony anatomy

Masi L.*, Pasciuti K.*, Doro R., Menichelli C.*, Polli C. *, Bonucci I. *, D'Imporzano E.*, Casamassima F.§. *Casa di Cura S.Chiara Florence Italy ;§U.O. di Radiobiologia Clinica University of Florence Italy

Introduction: Prediction of respiratory motion and accurate target localization are essential for free-breathing lung SRT. Positioning results by CBCT are reported: for target localization, the GTV from CBCT was matched to the ITV; matching based on the bony anatomy was considered for comparison. We analyzed the efficacy of patient training for reduction of breathing motion.
Materials and Method: Image-guided SRT was performed in 67 patients (91 lung malignancies). Two GTVs, delineated on end inhale and exhale CT data sets, were fused in an ITV. Tumor motion was evaluated as the displacement between these 2 phases. The PTV was the ITV plus a 3 mm margin. Using ABC spirometer (Elekta) for visual control and feedback, 28 patients were trained to maintain a regular breathing cycle, with a reduction of respiratory volume during the acquisition of simulation CT and CBCT, and treatment delivery. Before each fraction a CBCT was acquired and matched with the reference CT using bony structures. Thereafter the inclusion of the CBCT target inside the ITV was visually checked and, if necessary, further corrections performed obtaining the couch shift required for target alignment.
Results: Mean 3D tumor motion was 12.5 mm for mid and lower lobe lesions and 7.3 mm for upper lesions. Mean breathing displacements were lower for the patients trained to reduce respiratory volumes: respectively 6.2 mm and 3.8 mm for lower and upper lesions. The mean difference between the target and bone alignment using CBCT was 3.9 mm (SD=4.5 mm). In 30% of fractions the difference was <1 mm, but in 9% it exceeded 10 mm. Similar results were obtained for patients who had their breathing monitored by ABC.
Discussion: Bony anatomy as a surrogate of the target may lead to some relevant positioning errors, even if an ITV is created: target visualization on CBCT permits an accurate localization in lung SRT. Controlled reduction of respiratory volumes seems effective in reducing tumor motion.

Inter- and intrafractional movement of the tumour in extracranial stereotactic radiotherapy of NSCLC

Henrik R. Jensen#, Mogens Hjelm-Hansen#, Olfred Hansen*, Carsten Brink#,
#Laboratory of Radiation Physics, Odense University Hospital, DK-5000 Odense C, Denmark *Department of Oncology, Odense University Hospital, DK-5000 Odense C, Denmark

Introduction: The purpose of this study is to determinate the appropriate treatment planning margins related to inter- and intra-fractional respiration induced movements as well as setup accuracy in a stereotactic body frame a.m. Lax Blomgreen for stereotactic treatments of NSCLC patients.
Patients and methods: From August 2005 to January 2008, 17 patients with NSCLC where given a stereotactic treatment. The patients were scanned with normal and uncoached respiration without use of abdominal compression. Each patient had CT-scans performed at four occasions throughout the treatment: As part of the CT-simulation and before the 3 radiotherapy treatment. At every occasion six individual CT-scans covering the tumour volume were obtained. In this way 24 scans where obtained from each patient. In each CT-scan the maximum positions of the tumour where located in all 6 directions, represented by the top, bottom, anterior, posterior, left and right part of the tumour. These coordinate make up/constitute the data of this study. A common reference system between the individual CT sessions is obtained by fusion of the patient anatomy of a given CT session with the patient anatomy of the first CT session. Likewise a fusion of the body frame was performed to be able to measured patient positioning accuracy within the frame. All fusions was performed in the Syntegra module in the Pinnacle3 dose planning system.
Results: The standard deviations of the respiration induced intra-fractional movements were: LR: 0.8 mm, AP: 1.2 mm and CC: 2.2 mm (1 SD). The inter-fractional movements were: LR: 1.0 mm, AP: 1.3 mm and CC: 1.9 mm (1 SD). Finally the setup accuracies in the body frame were LR: 1.5 mm, AP: 1.1 mm and CC: 1.8 mm (1 SD). The standard deviation of the sum of all three uncertainties would be LR: 2.0 mm, AP: 2.1 mm and CC: 3.4 mm (1 SD).
Conclusion: With a patient fixated in a stereotactic body frame a.m. Lax Blomgreen, we conclude that large movements of the tumour are rarely seen within the lung. With consecutive scans, using a conventional CT-scanner, it is possible to find those patients in whom the tumour movement is large. The relative small respiration induced movements shows that gating will not be able to reduce treatment margins substantial. However 4D CT and Cone beam CT will be able to reduce the treatment margins.

Eva Brun

Salivary gland volume and dose in IMRT for head and neck cancer assessed using cone-beam CT

U. V. Elstrøm, S. Buus, L. P. Muren, J. B. Petersen, and C. Grau. Aarhus University Hospital, Department of Oncology and Department of Medical Physics, Denmark

Anatomic changes during radiotherapy can lead to deviations between planned and delivered dose distribution. The aim of the present study was to assess if cone-beam CT (CBCT) is feasible for quantification of anatomic and dosimetric changes as a step towards adaptive image-guided RT.
Consecutive head and neck cancer patients treated with dynamic parotid-sparing IMRT were enrolled. Weekly CBCT scans were compared to concurrent conventional CT scans, and with the planning CT to recalculate the original IMRT dose plan. Parotid and submandibular glands were contoured and volumetric, positional and dosimetric changes were determined. So far, a total of 92 CBCT/CT scans acquired from 15 patients have been analyzed.
Inter-observer variation in salivary gland contouring was studied by analyzing volumes delineated by six different physicians. A mean parotid volume of 40 cm3 (coefficient of variance, CV 9%) for CBCT compared to 36 cm3 (CV 13%) for CT ($p=0.002$) was found. Submandibular volumes were 9 cm3 (CV 20%) for CBCT compared to 7 cm3 (CV 17%) for CT ($p=0.03$). Intra-observer variation was studied by analyzing five repeated contour sets done by one physician. The data showed a mean parotid volume of 41 cm3 (CV 6%) for CBCT compared to 35 cm3 (CV 7%) for CT ($p=0.02$). Submandibular volumes were 10 and 8 cm3, with CVs of 15% and 12%, respectively. The data suggest that CBCT compared to CT overestimates the salivary gland volume by 15-20% and has insignificantly higher CVs.
During the six weeks of radiotherapy, the parotid volume changed, especially in glands receiving more than 20 Gy. The median volume reduction was 0.2 cm3 (0.7%) per day. Preliminary data indicate a modest increase in mean gland dose during treatment.
CBCT was feasible for measuring volume and dose changes in salivary glands during six weeks of IMRT. CBCT compared to CT overestimated the salivary gland volume by 15-20%, but with comparable inter-observer and intra-observer variability.

Daily volumetric image-guidance: Does routine usage prompt adaptive re-planning

J. Tanyi, W. D'Souza, M. Fuss, Radiation Medicine, Oregon Health & Science University, Portland, OR

Purpose: To investigate how the use of daily volumetric image-guidance using an on-board cone-beam CT system impacts on the frequency of adaptive re-planning.
Materials: Since July 2008, 146 patients have undergone a course of external beam radiation therapy using volumetric CBCT image-guidance. The frequency of image-guidance ranged from daily to once weekly. We assessed with which frequency adaptive re-planning was conducted and what was the cause of re-planning.
Results: In this population, 23% of patient plans were adapted to a changed anatomy at least once (up to 6 times) during their course of EBRT. Most common causes for adaptive planning were: tumor change (mostly shrinkage), change in abdominal girth, and weight loss. We will document significant consequences of changed anatomy on prescribed dosimetry. Exemplary cases of tumor change, girth change, and weight loss will be presented along with unusual adaptive scenarios (intestinal contrast accumulation following radiology exam, unexpected tumor location change).
Discussion: Routine use of volumetric image-guidance has in our practice increased the demand for adaptive re-planning. Daily CBCT image-guidance provides sufficient imaging information to reliably predict the need for dose adjustment, as in all cases studied, the initial and adapted dosimetry differed from each other.

Setup errors in patients undergoing image guided radiation treatment. Relationship to body mass index and weight loss

Johansen J.*, Bertelsen A.#, Hansen C.R.#, Westberg J.#, Hansen O.*, Brink C.#
*Department of Oncology, Odense University Hospital, DK-5000 Odense C, Denmark
#Laboratory of Radiation Physics, Odense University Hospital, DK-5000 Odense C, Denmark

Introduction: Treatment reproducibility during fractionated radiotherapy of head-and-neck cancer may be affected by factors such as tumor shrinkage, soft tissue edema, and body weight loss. The impact of BMI and weight loss on treatment setup errors was assessed by cone-beam CT (CB) imaging in a prospective study. Patients and Methods: Preliminary data from 34 consecutively treated head-and-neck cancer patients was analyzed. Patients were positioned in a vacuum fixation cushion and with a full thermoplastic face mask, and treated on an Elekta Synergy accelerator. CB acquisitions were obtained according to a standardized Action Limit protocol and compared to pre-treatment CT images. Patient position at treatment was determined using an automatic grey scale matching algorithm in a predefined volume (clip box) according to our set-up protocol for head-and-neck patients. The average 3D deviation from 3 initial cone-beam scans was compared to deviations at the 10th, 20th, and 30th treatment and correlated by linear regression analysis to BMI, height, and weight loss as expressed by the relative weight change over time. Body-weight was recorded weekly. Results: The median BMI at the beginning of treatment was 25.8 (17.6-39.7). The median weekly weight change was -0.3% (-2.0% to 1.1%). The standard deviation of the translational and rotational setup errors during the three first session were 0.9 mm (LR), 1.1 mm (AP), 0.7 mm (CC) and 0.7º (LR-axis), 0.5º (AP- axis) and 0.7º (CC- axis). The setup error at treatment session 10 was correlated to height, BMI, weight, weight change during treatment course and mean setup errors at session 1, 2 and 3. Only the initial setup showed to be significant. No correlation between the 20th or 30th session was found with the above stated parameters. Conclusion: Patient-related factors such as height, BMI, and weight loss during radiotherapy did not impact significantly on setup errors as assessed from 34 head-and-neck cancer patients. The present immobilization system has ensured a safe positioning during a course of radiation treatment within the limits of our planning margins. Due to previous studies indicating a relationship between weight loss and setup errors, and the lack of any such association in the present study, we are currently investigating similar data in lung cancer patients.

High-precision cone-beam CT-guided intra cranial stereotactic radiosurgery: Extensive quality assurance and clinical results

Præstegaard H L, Seiersen K, Elstrøm U V, Petersen J, Poulsen P R, Schultz H, Traberg A, and Høyer M. Department of Oncology, Aarhus University Hospital

Introduction: Since May 2007 our clinic has performed frameless intra-cranial stereotactic radiosurgery (SRS) using a cone-beam CT (CBCT) imaging system on-board the linear accelerator. In comparison with invasive frame-based SRS, CBCT-guided SRS has the benefit of good patient comfort, planning and treatment at separate days (similar to conventional radiotherapy), and the possibility of fractionated treatment.
Materials and methods: All individual geometrical errors for localizing a target with CBCT guidance have been carefully evaluated. In addition, the accuracy of the complete clinical process has been tested for a cranial phantom with natural human bony anatomy. At the treatment session, the patient is immobilized in a conventional head-and-neck mask system. After initial positioning using external landmarks, a CBCT dataset is acquired, providing automatic correction of the patient position. Following, the patient position is verified with a second CBCT scan, and a third CBCT scan after the treatment provides information about the intra-fraction motion. The intra-fraction motion is also monitored by cine MV imaging during treatment.
Results: All the individual geometrical errors of CBCT-guided SRS are small, resulting in a total random target localization error of only 0.6 mm along all axes (one standard deviation) in case of negligible intra-fraction patient motion. In addition, the systematic deviation between the CBCT isocenter and the radiological isocenter can be eliminated in the software. The treatment error of the cranial phantom is in excellent agreement with the sum of the individual geometrical errors. 8 patients with cranial metastases have been treated using CBCT guidance (March 2008) with an average treatment time of 55 minutes, and a minimum treatment time of 40 minutes for a non-coplanar treatment with 5 fields. The intra-fraction patient motion during treatment is below 1 mm along any axes for most patients.
Conclusion: High-precision intra-cranial SRS with CBCT guidance at the treatment session is feasible, efficient, comfortable for the patient, and the accuracy is comparable to invasive frame-based SRS. With more experience, faster software, and a new fixation with better clearance, the average treatment time is expected to decrease to 35-40 minutes.

The Future of IGRT - Cost Benefit Analysis

Michael Baumann & Daniel Zips, Dept. of Radiation Oncology, OncoRay Center for Radiation Research in Oncology and University Cancer Center, Medical Faculty and University Hospital Carl Gustav, University of Dresden, Germany

The aim of IGRT is to improve tumour coverage and spare normal tissues. Higher rates of local control and lower toxicitiy, without doubt, are of benefit for the patient. Treatment of failures or toxicities is often very expensive. Several additional parameters suggest a benefit of IGRT: The age of patients receiving radiotherapy is rapidly increasing, which, because of co-morbidity, may increase the risk of normal tissue damage. The same applies for multidisciplinary treatment which may increase the risk of cumulative toxicities. New molecular targeting agents, which might have little or even no notable antitumoral properties themselves, will be increasingly used to improve the curative potential of radio(chemo)therapy. Despite of their "selective" mechanisms, all targeted drugs will potentially increase the risk of normal tissue damage. Therefore clinical trials on new molecular approaches need very high-quality radiotherapy approaches to validate efficacy and safety. Future individualized radiotherapy will use biological imaging techniques that depict the biological features of the tumour in situ. Sophisticated IGRT techniques will be necessary for meaningful integration of such information into biologically adapted radiation treatments. Also the physical advantages of new beams (protons, ions) can only be translated into a benefit if combined with best planning and delivery techniques. IGRT appears a straightforward approach to improve radiotherapy. However, from a formal point of view, very little high level evidence has been provided by radiation oncologists that IGRT, which brings additional costs, is superior to more conventional and less costly radiotherapy techniques. Possible ways out of this dilemma are stringent adherence of the radiotherapy community to EBM principles when new technologies are assessed or development of dedicated principles for clinical technology assessment.

Broadening the scope of image-guided radiotherapy

Carlo Greco[a] and C. Clifton Ling[b], Departments of Radiation Oncology[a] and Medical Physics[b], Memorial Sloan Kettering Cancer Center, New York, New York, USA

The recent wave of enthusiasm for image guidance in radiation therapy is largely due to the advent of on-line imaging devices. The current narrow definition of image-guided radiotherapy (IGRT), in fact, essentially connotes the use of near real-time imaging during treatment delivery to reduce uncertainties in target position and should therefore be termed IGRT-D. However, a broader (and more appropriate) context of image-guidance should include: (1) detection and diagnosis, (2) delineation of target and organs at risk, (3) determining biological attributes, (4) dose distribution design and (5) dose delivery assurance and (6) deciphering treatment response through imaging i.e. the 6 D's of IGRT. Strategies to advance these areas will be discussed.

Evaluation of long-term changes in lung tumors by transit in-vivo dosimetry

A. Fidanzio[1], F. Greco[1], A. Mameli[1], L. Azario[1], L. Grimaldi[2], G. D'Onofrio[2], S. Cilla[2], B. Augelli[2], V. Valentini[4], A. G. Morganti[5], A. Piermattei[1,2.] [1]Istituto di Fisica – Università Cattolica S. Cuore (Roma).[2]U.O. Fisica Sanitaria –Università Cattolica S. Cuore (Campobasso).[3] U.O. Radioterapia – Università Cattolica S. Cuore (Roma).[4] U.O. Radioterapia –Università Cattolica S. Cuore (Campobasso)

Introduction: The long-term changes in tumor configuration is one of the problems that can be investigated by the Electronic Portal Image (EPI) to perform image guided radiotherapy. In this work using the EPI, an in-vivo dosimetry is applied to check treatments of lung tumors where modifications of the tissues during the therapy can occur. The dosimetric information can help the radiation oncologist to decide when new CT scan and new re-planning have to be carried out. Materials and methods: The in-vivo dosimetry method (that can be used in tissue inhomogenety regions) is based on correlation functions obtained by the ratios between the transit signals, St, and the mid-plane doses, Dm, measured in solid water phantoms of different thicknesses. The method was implemented in different centers to reconstruct the isocenter dose, Diso, in the patient. The signals St were obtained by an aS-500 Elettronic Portal Imaging Device (EPID). A tolerance-action level equal to 5% was used for lung treatments. Three patients with lung cancer were checked with the in-vivo dosimetry method. When the ratio R between the in-vivo reconstructed isocenter dose, Diso, and the treatment planning system (TPS) dose, Diso,TPS, showed values systematically out of the tolerance level, a new patient's TC scan was acquired to verify the tumor morphology. Results: The three patients showed R values systematically out of the tolerance level and dosimetric variations up to 10% were observed after 15-20 Gy. For all the cases the radiation oncologist decided to continue the treatment with the same beams and monitor unit numbers to ensure the sterilization of the sub clinical disease of the initial target. However the new CT scans were used to determine the hybrid plan and the R values calculated with the new Diso,TPS values were well within the tolerance level. The analysis of the dose volume histograms by the two set of CT scans showed, for one patient, significant differences. Conclusions: On the basis of these results the radiation oncologists are planning to repeat the CT scans when the disagreement between the reconstructed and planned dose is out of tolerance level.

Experience with daily online image-guided positioning in radiotherapy

Martin Skovmos Nielsen, Jane Nielsen og Jesper Carl. Department of Medical Physics, Oncology, Aalborg Sygehus

The possibility to give external beam radiotherapy with reduced margins has emerged during the last years. Various techniques are available such at portal imaging, cone beam CT and stereo X-ray.
The use of daily online image guided positioning using stereo X-ray imaging was implemented in the department using the Exactrac system with Robotics from Brainlab. At present time the technique has been applied to all patients groups receiving treatment in the pelvic, Head and Neck (H&N) and cranial regions. Match between reference DRR images from the treatment plan and stereo X-ray images are mainly based on the bony anatomy. For prostate cancer patients, match on internal fiducial markers are used. Geometric precision in the Exactrac system is very good. Independent checks using portal imaging demonstrated spatial precision in the range 0.2 – 0.3 mm. Intra fraction movements however deteriorates this with a factor of ten, limiting margins to no less that 3-4 mm. The use of Robotics has the potential to reduce margins further compared to translation only. Rotation with Robotics however is limited to pitch: +/- 2.5 degree roll: +/- 4 degree yaw: +/- 3 degree. Rotations will often fall within these limits for treatment using match on the bony anatomy. Couch sag or bending of attached H&N support may present a problem in Head or Cranial region. Care should be taken to reduce these effects by ensuring a good stability in the couch. For matching on internal organs as the prostate the situation differs. Difference in rectal filling, or gas, between fractions may introduce rotations of the prostate that exceeds the limits of Robotics with more than 10 degree. Consequently the advantage of using Robotics may be offset. In cases where large rotations of the prostate are present in the planning CT, systematic errors may be introduced into the treatment plan. This implies that care should be taken to evaluate the planning CT for excessive rotation of the prostate. In such cases the rectal filling should be cleared and a new planning CT performed.

Multimodality imaging in radiation treatment planning for carcinoma of the nasopharynx: a sub-volume analysis

Fowler, A; Forstner, D; Lin, P; Cuganesan, R; Clark, J. Liverpool Hospital, Sydney, Australia

Introduction: Conventional radiation treatment planning relies on visual interpretation of CT images to define a gross tumour volume (GTV). A combination of CT, MR, and FDG-PET imaging may be useful in defining a more accurate GTV provided that the increased information available can be processed in a structured and coherent manner.
Materials and Methods: The images of 32 year old female patient with T2N2 nasopharyngeal carcinoma were reassessed following treatment. GTV-CT and GTV-MR were delineated visually. GTV-PET was defined as the volume of tissue in the nasopharyngeal region with a Standardized Uptake Value (SUV) or 2.5 or greater. The three images sets were fused and volumetric comparisons performed. Volumes of tissue were defined according to whether 1, 2 or 3 modalities were indicative of tumour at a given location. If tissue was contoured as part of the GTV on any of the modalities this was defined as GTV-(1 modality). The volume of tissue that was contoured as tumour on all 3 modalities was defined as GTV-(3 modality). An intermediate volume, GTV-(2 modality) contained tissue that was positive for tumour for any 2 of the 3 imaging modalities.
Results: The delineated volumes for GTV-CT, GTV-MR and GTV-PET were 41.1cm3, 32.3 cm3and 49.7cm3 respectively. 60.5cm3 of tissue was suggestive of tumour on at least 1 of the three modalities – GTV-(1 modality). 41.3cm3 of tissue was designated as tumour on at least 2 modalities – GTV-(2 modality). 24.3 cm3 of tissue was defined as GTV on all 3 modalities- GTV-(3 modality).. The conformality index (volume of intersection divided by volume of union) between GTV-CT and GTV-(2 modality) was 0.70.
Discussion: The usefulness of MR and PET images for radiation treatment planning results from them being an inexact match for a CT defined GTV. However the additive GTV-(1 modality) volume is likely too large to be clinically useful. Conversely the restrictive GTV-(3 modality) is small and risks excluding tumour. GTV-(2 modality) is similar in size to individual volumes and may represent a useful starting point in defining a clinically relevant multimodality GTV.

Localization of the prostate in patients with prostate cancer with three different imaging methods

Á. Logadóttir, S. Korreman, M. Enmark. Department of Radiation Oncology, Rigshospitalet, Copenhagen, Denmark

Introduction: The aim of the study is to investigate the possibility of locating the prostate daily directly using a ConeBeam CT (CBCT) in patients in treatment for prostate cancer. The uncertainties in connection with the use of three imaging methods, ExacTrac (BrainLab) and two different On-Board-Imaging (OBI) systems (Varian) available at Rigshospitalet in Copenhagen are also studied. At present the patient-setup prior to treatment is performed by taking two kV images from definite angles. Before the treatment starts gold seeds are implanted in the prostate to help localizing it on the images. Images are taken before each treatment fraction to make sure that the prostate is in the isocenter. It would be an improvement of the treatment if the prostate could be located with the CBCT with the same accuracy as today without the seed inserted.
Methods: At Rigshopitalet treatment rooms are equipped with an ExacTrac system and accelerators with OBI. This gives the opportunity to compare the uncertainties of three imaging methods directly. 1.X- ray images at definite angles (ExacTrac) 2.X-rays images where the angles can be chosen freely (OBI) 3.A volumetric image (CBCT) The study is carried out in two parts, one using a phantom and one with a group of patients. In the phantom study the uncertainties and doses for the three methods will be estimated and compared. In the second part all three methods will be used to localize the prostate for a selection of patients. For CBCT the localization will be performed with and without the markers. This will allow an estimate of the validity of using markers as a substitute for the prostate position.
Results and Discussion: It can be discussed if this gives the real picture of the prostate location in the body as the seeds might move with respect to the prostate. It would therefore result in a better treatment if it would be a possible to localize the prostate directly. CBCT scan taken in connection with each fraction can make this an option. As long as the CBCT without the markers is precise enough it will not be necessary to operate the patients to implant the seeds. Preliminary results from the phantom study indicate that all three methods have a similar accuracy. The uncertainty is around 1 mm in all directions for all three modalities. The next step is to use all the imaging methods on prostate patients at Rigshospitalet.

Early clinical experience using implanted fiducial markers and daily online isocenter setup correction in prostate cancer radiotherapy

Ghazwan Al-Haidari, Jon Brinchmann Reitan, Dag Clement Johannessen and Ståle Ølberg. The Cancer Centre, Ullevål University Hospital, Oslo, Norway

In October 2007 we implemented the use of fiducial markers to the prostate gland as a guide to increase the precision of radiation and to reduce the dose to organs at risk. Numerous studies are describing different margins to the CTV by image guided radiotherapy (IGRT). As methods and equipment differs between centers it is of importance to define local setup errors in our institution. The aim of this preliminary study is to evaluate the accuracy of our IGRT method by describing the interfractional deformation, rotation and translation of the organ. This will subsequently, with a larger scale of patients, help to decide local total treatment margins. Gold seeds were implanted in 20 cancer prostate patients at least one week before the planning CT scan, two markers placed in the base (right and left) and one placed in the apex of the prostate. A total dose of 70 to 78 Gy was delivered in 35 to 39 fractions, respectively, by use of daily image-guided on-line position correction. The field setup was verified and corrected with two orthogonal kV images (anteroposterior & lateral) before each fraction. By skin marks positioning of the patients the images were matched in relation to bony structures to find the setup margins. In addition the gold markers were matched in respect to the markers in corresponding DRRs. The position of each marker was logged for each patient and fraction. The centre of mass and the plane defined by the three markers was calculated and used to find the daily variation of the prostate rotation and translation. The results will be presented in a poster.

Stereotactic body radiotherapy for medically inoperable stage I non-small cell lung cancer: mature outcome and toxicity results

Kopek N, Paludan M, Petersen J, Grau C, Høyer M. Department of Oncology, Aarhus University Hospital, Aarhus, Denmark

Purpose: To report the mature outcome and toxicity results of stereotactic body radiotherapy (SBRT) in the treatment of medically inoperable patients with primary stage I NSCLC at the Aarhus University Hospital.
Methods: Between 2000 and 2007, 89 consecutive patients were treated by linac-based SBRT using a body frame. Forty-five gray in three fractions (BED 112.5 Gy) over one week prescribed to the isocentre was given until 2004 when 67.5 Gy in 3 fractions (BED 219.4 Gy) was introduced for non-centrally located lesions. Forty-six percent of patients were under protocol while the remainder were retrospectively reviewed.
Results: With a median follow-up of 44 months, 5 patients developed local failure. The local control rate at 4 years was 89% while the freedom-from-failure was 36%. The 2-,3- and 5-year cancer specific survival was 72%, 64% and 50% respectively, with a median of 61 months. The median overall survival was 22 months. No significant differences in control or survival rates were observed between dose schedules. Seventy-eight percent of all worst toxicity grade scores were grade 0 or represented no change from baseline. Of all toxicities above baseline, the most frequent was asymptomatic pulmonary fibrosis (20.4%), followed by worsening of performance status (14%) and dyspnea (11.7%). Most toxicity was grade 1 (67.9%) with 14% grade 3/4. This profile was consistent during both the acute/subacute and late onset periods, with the exception of the most frequent toxicity: asymptomatic pneumonitis dominated the subacute period progressing to fibrosis in the late period. No significant difference in overall toxicity profiles were observed between dose schedules.
Conclusion: Longer follow-up confirms the excellent local control and encouraging survival outcomes of SBRT for inoperable early stage NSCLC. The late toxicity is characterized by radiographic changes and decline in lung function/PS. No significant gain in control with a BED > 112.5 Gy was observed and therefore use of a lower dose/fraction schedule for centrally located lesions is recommended. SBRT is now the standard of care for inoperable stage I NSCLC at Aarhus University Hospital.

A video-fluorscopic analysis of liver respiratory motion using fiducial markers to measure effectiveness and reproducibility of motion reduction by abdominal compression

Wunderink, W. M.Sc.,* Mendez Romero, A. M.D.,*de Kruijf, W. Ph.D.,* de Boer, J. Ph.D.,* Levendag, P. M.D., Ph.D.,* and Heijmen, B. Ph.D.* *Erasmus Medical Center–Daniel den Hoed Cancer Center, Rotterdam, The Netherlands

Purpose: To measure the reduction and reproducibility in respiratory liver motion that can be achieved using abdominal compression in a stereotactic body frame.
Methods and Materials: A video fluoroscopy system was used to measure the excursion of gold fiducial markers implanted in the liver of 12 patients. Fluoroscopic videos were acquired on the planning day and before each treatment fraction using various levels of abdominal compression, and free-breathing. By including a force transducer in the compression plate, we measured the varying force exerted by the plate on the patient's abdomen. We compared force against screw position to determine their suitability as a reference for the treatment's compression set-up.
Results: In 10 patients the top-top craniocaudal (CC) respiratory excursion was reduced below 5mm. Excursions measured in left-right (LL) and anterioposterior (AP) directions were below 5mm in all 12 patients. The median residual excursions were 4.1 mm CC, 2.4 mm LR, and 1.8 mm AP. The median reproducibility of the residual excursions were 0.7 mm CC, 0.2 mm LR, 0.6 mm AP (1 standard deviation). Residual respiratory CC motion on treatment days was never significantly (α = 0.05) greater than on the planning days. Fine-tuning of the compression level did not considerably change the excursion on the treatment days. Abdominal force was, compared to screw position, not a better reference for setting up the compression level. However, force measurements were useful to monitor the breathing activity.
Conclusion: Abdominal compression was effective in reducing liver motion, yielding small and reproducible excursions in three dimensions. Tumor margins could be based safely on the video-fluoroscopic measurements of residual motion performed on the planning day, suggesting treatment day verifications are unnecessary.

Gated radiotherapy of lung cancer: interfractional changes in tumor volume and position during the treatment course

T. Juhler-Nøttrup, A.N. Pedersen, S.S. Korreman, N. Plougmann, L.R. Aarup, H. Nyström, L. Specht. The Finsen Center, Radiotherapy, Copenhagen, Denmark.

Background: With the purpose of implementing IGRT for lung cancer patients undergoing curative radiotherapy for locally advanced disease, this study investigated the interfraction variations in tumor size and internal displacement with the use of respiratory gating. The variations were compared for different set up strategies.
Methods and Materials: During their treatment course, the included patients underwent 3 respiratory gated CT-scans, equally spaced in time. The tumors were contoured on each CT-scan to evaluate the variation in volume and position. The primary lung tumors and the mediastinal tumors were contoured separately. The positional variations were measured as 3D mobility vectors and related to matching of the scans on the basis of bony landmarks and with skin tattoos.
Results: The mean 3D mobility vector and the SD for the lung tumors was 0.51 cm (0.21) for matching performed with bony landmarks and 0.85 cm (0.54) for matching with skin tattoos. For the mediastinal tumors the corresponding vectors and SD's were 0.55 cm (0.19) and 0.72 cm (0.43). The differences between the vectors were significant for the lung tumors. The mobility vectors for the tumors in the lung and the mediastinum were not comparable for each patient. There was a significant reduction in tumor size from the first to the last CT-scan. For the lung tumors the reduction was 19% and for the mediastinal tumors the reduction was 34%. The interfractional overlap of lung tumors was 80-87% when matched using bony landmarks and 70-76% when matched using skin tattoos. The overlap of the mediastinal tumors were 60-65% and 41-47%, respectively.
Conclusions: Despite the use of gating the tumors varied considerably, regarding both position and volume. The variations in position were dependent on the set up strategy. Set up using IGRT was superior to set up using skin tattoos. Even using IGRT margins are mandatory.

Three-dimensional set-up errors assessment in post-operative head and neck radiotherapy using electronic portal imaging device.

Gupta T, Chopra S, Kadam A, Agarwal JP, Devi PR, Ghosh-Laskar S, Dinshaw KA. Departments of Radiation Oncology, Advanced Centre for Treatment Research and Education in Cancer & Tata Memorial Hospital, Mumbai, India

Background: Set-up errors, though undesirable are an inherent part of the radiation treatment process. The coverage of target volume is a direct function of set-up margins, which should be optimized to prevent inadvertent irradiation of adjacent normal tissues. The aim was to evaluate three-dimensional (3D) set-up errors and propose optimum margins for target volume coverage in post-operative head and neck radiotherapy.
Methods: The dataset consisted of 93 pairs of orthogonal simulator and corresponding portal images on which 558 point positions were measured to calculate translational displacement in 25 patients undergoing post-operative head and neck radiotherapy with antero-lateral wedge pair technique. Mean displacements, population systematic (Σ) and random (σ) errors and 3D vector of displacement were calculated. Set-up margins were calculated using published margin recipes.
Results: The mean displacement in antero-posterior (AP), medio-lateral (ML) and supero-inferior (SI) direction was -0.25 mm (-6.50 to +7.70 mm), -0.48 mm (-5.50 to +7.80 mm) and +0.45 mm (-7.30 to +7.40 mm) respectively. Ninety three percent of the displacements were within 5 mm in all three cardinal directions. Population systematic (Σ) and random errors (σ) were 0.96, 0.98 and 1.20 mm and 1.94, 1.97 and 2.48 mm in AP, ML and SI direction respectively. The mean 3D vector of displacement was 3.84 cm. Using van Herk's formula, the clinical target volume to planning target volume margins were 3.76, 3.83 and 4.74 mm in AP, ML and SI direction respectively.
Conclusion: The set-up margins were <5 mm in all directions and is in concurrence with other published literature of set- up errors in curative head and neck radiotherapy practice. Caution is warranted against adopting generic margin recipes as different margin generating recipes lead to a different probability of target volume coverage.

Participants (updated per 22. May 2008)

Agarwal Jai Prakash
Department of Radiation Oncology
Tata Memorial Hospital
Dr.E Borges Road, Parel
Mumbai 40012
India

Aguilar Manuel
Regional Manager Scandinavia
BrainLAB Sales GmbH
Kapellenstr. 12
Feldkirchen 85622
Germany

Ahlén Natalie
Marketing and Sales
SAM Nordic
Östmarksgatan 27
Farsta 12342
Sweden

Ahlén Seija
Sales
SAM NORDIC
Östmarksgatan 27
12342 Farsta 12342
Sweden

Akeab Imad
Astronomy
Baghdad University
Iraq/baghdad/Aljadreeah
baghdad 964
Iraq

Alber Markus
Section for Biomedical Physics
Clinic of Radiooncology, University of Tübingen
Hoppe-Seyler-Street 3
Tübingen 72076
Germany

Alhaidari Ghazwan
Cancer Centre
Ulleval University Hospital
Kirkegate
Oslo 407
Norway

Andersen Lisbeth Juhler
Department of Oncology
Aalborg Sygehus
Hobrovej 18-22
Aalborg 9100
Denmark

Arriagada Rodrigo
Radiotherapy
Karolinska Institutet
Radiumhemmet c/o Pia Bulow
Stockholm 0
Sweden

Bak Mogens
Rad.fys.52AA
Herlev Hospital
Herlev Ringvej 75
Herlev 2730
Denmark

Balducci Mario
Radiotherapy
Policlinico A.Gemelli UCSC
largo A.Gemelli 8
Roma 168
Italy

Bangsgaard Jens Peter
Afd. for Medicinsk Fysik
Vejle Sygehus
Kabbeltoft 25
Vejle 7100
Denmark

Baumann Michael
Dept. of Radiotherapy and Radiation Oncology
Technical University of Dresden
Fetscherstraße 74
Dresden 0
Germany

Behrens Claus F
Oncology
Herlev Hospital
Herlev Ringvej 75
Herlev 2730
Herlev

Bentzen Lise
Dept. of oncology
Aarhus University Hospital
Norrebrogade 44
Aarhys C 8000
Denmark

Bonomo Pierluigi
Radioterapia
Policlinico A.Gemelli UCSC
Largo A.Gemelli 8
Rome 168
Italy

Brink Carsten
Laboratory of Radiation Physics
Odense University Hospital
Sdr. Boulevard 29
Odense C
Denmark

Brock Kristy
Radiation Oncology
Princess Margaret Hospital
610 University Ave, Rm 7-502A
Toronto
Canada

Brun Eva
Oncology
Oncology
University Hospital
Lund
Lund

Busk Morten
Department of Exp Clinical Oncology
Aarhus University Hospital
Noerrebrogade 44
Aarhus 8000
Denmark

Byberg David
Radiation Therapy
Stavanger University Hospital
P.O.Box 8100
Stavanger 4068
Norway

Bøje Charlotte
Dep. of Oncology
Århus Sygehus
Nørrebrogade
Århus 8000
Denmark

Bøjen Annette
Department of Oncology
Aarhus University Hospital
Nørrebrogade 44
Aarhus C 8000
Denmark

Carl Jesper
Dept Medical Physics
Oncology, Aalborg hospital
Hobrovej 18-22
Aalborg 9240
Denmark

Carlström Karl-Erik
Sales
IBA Particle Therapy
Strandbodsgatan 1, Box 1004
Uppsala 75140
Sweden

Cilla Savino
U.O. Fisica Sanitaria
Università Cattolica S.C.
Largo Gemelli 1 Cont. Tappino
Campobasso 86100
Italy

Cirino Gianni
Medical Physics
Univ Tor VERGATA
Via Montpellier, 1
Roma 133
Italy

Dasu Alexandru
Department of Radiation Physics
Norrland University Hospital
Umeaa University
Umeå
Sweden

Djärv Emma
Dep. of Radiation Therapy
MFT Terapeutisk Radiofysik
Gula stråket 2B
Göteborg
Sweden

Duus Anja
Department of Oncology
Aarhus University Hospital
44 Norrebrogade
Aarhus 8000
Denmark

Eilertsen Karsten
Department of medical physics
The Norwegian Radium Hospital
Montenbello
Oslo
Norway

Elstrøm Ulrik Vindelev
Dept. of Oncology
Aarhus University Hospital
Nørrebrogade 44, bygn. 5
Århus C 8000
Denmark

Eriksson Andreas
BrainLAB
BrainLAB Sales GmbH
Kapellenstr. 12
Feldkirchen 85622
Germany

Evensen Jan Folkvard
Dep of oncology
Norwegian Radium Hospital
Montebello
Oslo 310
Norway

Fenkell Louis
Radiation Oncology
Arhus University Hospital
44 Norrebrogade
Aarhus 8000
Denmark

Fidanzio Andrea
Istituto di Fisica
Università Cattolica S.C.
L. F. Vito 1
Rome 168
Italy

Fiorino Claudio
Medical Physics
San Raffaele Institute
Via Olgettina 60
Milano 20132
Italy

Fisker Rune Vincents
Dept. of Radiology
Aalborg Hospital
Hobrovej 18-22
Aalborg 9100
Denmark

Fode Kirsten
Oncology
NBG, Aarhus
Nørrebrogade 44
Aarhus 8000
Denmark

Forsberg Robert
Radeq
Radeq
Box 20103
Stockholm 10460
Sweden

Fowler Allan
Cancer Therapy
Liverpool Hospital
Elizabeth Drive
Sydney 2170
Australia

Franklin Peter
Medicinsk Fysik
Vejle Sygehus
kabbeltoft 25
Vejle 7100
Denmark

Fuss Martin
Radiation Medicine
Oregon Health & Science University
3181 SW Sam Jackson Park Rd
Portland, OR 97239
USA

Gauffin Clara
RadeqAB
RadeqAB
Hornsgatan 74 pobox 201 03
Stockholm
Sweden

Gauffin Johan
Radeq AB
Radeq AB
Hornsgatan 74A
Stockholm 11821
Sweden

Geerlof Erik
Sales
Elekta Instrument AB
De Maas 26
Best, Noord-Brabant 0
Netherlands

Geleijns Jacob
Radiology
LUMC
Albinusdreef 2
Leiden
The Netherlands

Ghane Hadi
Sales/R&D
Beampoint AB
Kista Science Tower
Kista, Stockholm 16451
Sweden

Granlund Ulf
Dept of Medical Physics
Örebro University Hospital
Örebro University Hospital
Örebro
Sweden

Grau Cai
Department of Oncology
Aarhus University Hospital
44 Norrebrogade
Aarhus 8000
Denmark

Hansen Jolanta
Medical Physics
Aarhus University Hospital
44 Norrebrogade
Aarhus 8000
Denmark

Hansen Katarina
Exhibitor
Par Scientific A/S
Sivlandvaenget 11B
Odense S 5260
Denmark

Hansen Steinbjørn
Oncology
Odense University Hospital
Sdr Boulevard
Odense 5000
Denmark

Hansen Vibeke Nordmark
Joint Physics Department
Royal Marsden NHS Trust and Institute of Cancer Research
Downs Road, Sutton, Surrey 0
United Kingdom

Haustermans Karin
Radiation Oncology
Leuven Cancer Institute, University Hospital
Herestraat 49
Leuven 3000
Belgium

Havsteen Hanne
Department of Oncology R
Herlev
Herlev Ringvej 75
Herlev 2730
Denmark

Hoffmann Axel
Sales
PTW-Freiburg
Loerracher Str. 7
Freiburg 79115
Germany

Hoffmann Lone
department of oncology
medical physics
Noerrebrogade 44
Aarhus 8000
Denmark

Holm Søren
PET 3982
Rigshopitalet
Blegdamsvej 9
København
Denmark

Hornsleth Sten
Varian Medical Systems
Lyskær 9
Herlev 2730
Denmark

Hoyer Morten
Dept. Oncology
Aarhus University Hospital
Norrebrogade 44
Aarhus C 8000
Denmark

Haack Søren
Dept. of Biomedical Engineering
Aarhus University Hospital
c/o AUH Skejby - Brendstrupgaardsvej
Aarhus N 8200
Denmark

Iyer Victor
Nuclear Medicine
Aalborg University Hospital
Hobrovej
Aalborg 9000
Denmark

Jensen Helle Anita
dept. of oncology
Odense Universitetshospital
Sdr. Boulevard 29
5000 Odense C 5000
Denmark

Johannessen Dag Clement
Oncology
Ullevål universitetssykehus
Kirkeveien 166
Oslo
Norway

Johansen Jørgen
Department of Oncology
Odense University Hospital
Sdr. Boulevard 29
Odense C
Denmark

Jolinder Eva
Sales Operations
BrainLAB Sales GmbH
Kapellenstr.12
Feldkirchen 85622
Germany

Jordeby Lars
C-RAD Positioning AB
C-RAD Positioning AB
Bredgränd 14
Uppsala 75320
Sweden

Juhler-Nøttrup Trine
Oncology
Herlev Hospital
Grøndals Parkvej 92 st.
Vanløse 2720
Denmark

Kandi Maria
Oncology
Aarhus university Hospital
Nørrebrogade 44
Århus 8000
Denmark

Kessler Marc
Radiation Oncology
The University of Michigan
519 W William
Ann Abor 48103
USA

Khalil Azza
Oncology
Aalborg Sygehus
Rønnehaven 75
Lystrup 8520
Denmark

Kjær-Kristoffersen Flemming
Radioterapiklinikken
Rigshospitalet
Blegdamsvej 9 - 3994
København Ø 2100
Denmark

Klitgaard Dorte
Rad.fys. 52AA
Herlev Hospital
Herlev Ringvej 75
Herlev 2730
Denmark

Kopek Neil
Oncology
Aarhus
Nørrebrogade 44, building 5
Aarhus 8000
Denmark

Korreman Stine
Dept. of Radiation Oncology
Rigshospitalet
The Finsen Centre, section 3994,
Blegdamsvej 9
Copenhagen, Denmark

Koszewska-Flejmer Anna
Department of Radiation Oncology
Linköping University
Linköping
Linköping
Sweden

Kuttner Samuel
Kreftavdelingen, Stråleterapi
Universitetssykehuset Nord-Norge
Postboks 17
Tromsø 9038
Norway

Kylling Arve
Dept. of Oncology
Ålesund hospital
Ålesund sjukehus
Ålesund 6026
Norway

Langkjer Sven
Dept of Oncology
Vejle Sygehus
Kabbeltoft 25
Vejle 7100
Denmark

Larsen Anders Christian
Surgical Gastroenterology A
Aalborg hospital
Hobro vej 18-22
Aalborg
Denmark

Larsson Peter
Radiation Physics
IMH
Linköping University Hospital
LInköping
Sweden

Li Gloria C
Medical Physic and Radiation Oncology
Memorial Sloan-Kettering Cancer Center
1275 York Avenue, Box 72
New York 10065
USA

Lind Mårten
Radiofysik
Universitetssjukhuset i Lund
Klinikgatan 7
Lund 22185
Sweden

Lindegaard Jacob Chr.
Department of Oncology
Aarhus University Hospital
44 Norrebrogade
Aarhus 8000
Denmark

Lindmo Tore
Physics
NTNU
Høgskoleringen 5
Trondheim 7491
Norway

Ling C Clifton
Department of Medical Physics
Memorial Sloan-Kettering Cancer Center,
1275 York Ave
New York 10021
USA

Linnet Nielsen Anni
Dept. of Oncology
Herlev Hospital
Herlev Ringvej 75
Herlev 2730
Denmark

Logadóttir Áshildur
Department of Radiation Oncology, 3994
Rigshospitalet
Blegdamsvej 9
Copenhagen 2100
Denmark

Mackie Rock
Dept of Human Oncology
University of Wisconsin
600 Highland Avenue
Madison
USA

Malinen Eirik
Department of Medical Physics,
Rikshospitalet University Hospital
Montebello
Oslo 310
Norway

Mansour Sayed
Medical physics
MPTS
P.O.Box 126
Brooklyn NY 11220
USA

Marthinsen Anne Beate L.
Department of Oncology
St. Olavs Hospital
Olav Kyrresgt. 17
Trondheim 7006
Norway

Masi Laura
Medical Physics department
Casa di Cura S.Chiara
Piazza Indipendenza 11
Firenze 50129
Italy

Medin Joakim
Radiation Oncology
Copenhagen Univ. Hospital
Blegdamsvej 9
Copenhagen 2100
Denmark

Mejlholm Inge
Department of Oncology
Vejle Sygehus
Kabbeltoft
Vejle 7100
Denmark

Miccichè Francesco
Radioterapia
Policlinico A.Gemelli UCSC
Largo A.Gemelli 8
Rome 168
Italy

Morgan Prof Graeme
Department of Radiation Oncology
Royal North Shore Hospital
Sydney
NSW 2065
Australia

Muren Ludvig
Dept of Medical Physics
Aarhus University Hospital
Nørrebrogade 44, Building 5
Aarhus 8000
Denmark

Myrdal Gardar
Radiation Physics
Landspitali
Hringbraut
Reykjavik 101
Iceland

Møller Søren
Sales
Varian Medical Systems
Lyskær 9
Herlev 2730
Denmark

Maad Kristofer
C-RAD Positioning AB
C-RAD Positioning AB
Bredgränd 14
Uppsala
Sweden

Nailon Bill
Oncology Physics
Edinburgh Cancer Centre
Western General Hsopital
Edinburgh
United Kingdom

Nielsen Jane
Afd.f.Medicinsk Fysik
Aalborg Sygehus Syd
Hobrovej 18-22
Aalborg 9000
Denmark

Nielsen Martin
Department of medical physics
Aalborg Hospital
Hobrovej 18-22
Aalborg 9100
Denamrk

Nielsen Thomas
Department of Exp Clinical Oncology
Aarhus University Hospital
Noerrebrogade 44, Building 5,2
Aarhus 8000
Denmark

Nilsson Per
Department of Oncology
Umeå University Hospital
Department of Oncology
Umeå
Sweden

Noe Karsten
Department of Computer Science
University of Aarhus
Aabogade 34
Aarhus N 8000
Denmark

Nordsmark Marianne
Oncology
Aarhus University Hospital
Nörrebrogade 44 bldg 5
Aarhus 8000
Denmark

Nutting Christopher
Dept of Radiotherapy, Head & Neck Unit
Royal Marsden Hospital
203 Fulham Road
London
United Kingdom

Nybø Tone
Dept.of Oncology and Medical Physics
Haukeland University Hospital
Jonas Lies vei 65
Bergen
Norway

Nygaard Ditte Eklund
Oncology
Rigshospitalet
Blegdamsvej
2100 0
Denmark

Nygaard Kirsten
Dept of Oncology and Medical Physics
Haukeland University Hospital
Jonas Liesvei 65
Bergen 5021
Norway

Nyvang Gitte-Bettina
Oncological dept.
Århus University Hospital
Nørrebrogade 44
Århus 8000
Denmark

Nørrevang Ole
Department of Medical Physics
Århus Universitetshospital, Århus Sygehus
Nørrebrogade 44, bygning 5J, 2. sal
Århus 8000
Denmark

Offersen Birgitte
Oncology
Aarhus University Hospital
Nørrebrogade 44
Aarhus C 8000
Denmark

Olsen Dag Rune
Dept of Medical Physics
Rikshospitalet-Radiumhospitalet
Montebello
Oslo 310
Norway

Overgaard Jens
Experimental Clinical Oncology
Aarhus University Hospital
44 Norrebrogade
Aarhus 8000
Denmark

Palmans Hugo
Radiation Dosimetry
National Physical Laboratory
Hampton Road
Teddington
United Kingdom

Pedersen Erik Morre
Dept. Radiology
Århus Sygehus
Nørrebrogade 44
Århus C 8000
Denmark

Persson Gitte
Radioterapiklinikken 3994
Rigshospitalet
Blegdamsvej 9
Copenhagen 2100
Denmark

Petersen Jørgen
Medical Physics
Aarhus University Hospital
44 Norrebrogade
Aarhus 8000
Denmark

Pettersen Petter A.
Radiotherapy
UNN
Boks 13
Tromsø 9038
Norway

Piermattei Angelo
Istituto di Fisica
Università Cattolica S.C.
L. F. Vito 1
Rome 168
Italy

Pløen John
Oncology
Vejle Sygehus
Kabbeltoft 25
Vejle 7100
Denmark

Poulsen Per Rugaard
Department of Oncology
Aarhus University Hospital
44 Norrebrogade
Aarhus 8000
Denmark

Primdahl Hanne
Department of oncology
Aarhus University Hospital
Nørrebrogade 44
Aarhus 8000
Denmark

Præstegaard Lars Hjorth
Department of Oncology
Aarhus University Hospital
Nørrebrogage 44, bygning 5J, 2. sal
Århus 8000
Denmark

Pötter Richard
Dept of Radiotherapy
Medical University of Vienna
Waehringer Guertel 18-20
Vienna
Austria

Redpath Tony
Oncology Physics
Edinburgh Cancer Centre
Western General Hospital
Edinburgh 0
United Kingdom

Rydin Martin
Onkologikliniken
Centralsjukhuset
Rosenborgsgatan
Karlstad 65185
Sweden

Rzepecki Jan
Onkologiska Kliniken
Universitetssjukhuset
Hospital Area
Linköping
Sweden

Rødal Jan
Dept. of Medical Physics
The Norwegian Radium Hospital
Kreftklinikken, Montebello
Oslo 0
Norway

Røe Kathrine
Department of Radiation Biology
Rikshospitalet University Hospital
Montebello
Oslo 310
Norway

Røhl Lisbeth
Radiology
Aarhus University Hospital
Nørrebrogade 44
Århus C 8000
Denmark

Rønde Heidi Staghøj
Aarhus University
Department of Physics and Astronomy
Trøjborgvej 66, 3. tv.
Aarhus C 8000
Denmark

Rösth Bengt-Eric
Sales
Elekta Instrument AB
Box 7593
Stockholm
Sweden

Sastre-Padro Maria
Radiation Physics
Rikshospitalet
Montebello
Oslo 310
Norway

Scheib Stefan
Imaging Laboratory
Varian Medical Systems
Taefernstrasse 7
Baden-Daettwil 5405
Switzerland

Schiappacasse Luis
Tomotherapy & Radiotherapy Unit
Clinica La Milagrosa
Modesto Lafuente, 14
Madrid 28010
Spain

Seiersen Klaus
Department of Oncology
Aarhus University Hospital
Nørrebrogade 44, bygn. 5, 2.
Århus C 8000
Denmark

Sjöström David
Division of Radiophysics (51AA)
Department of Oncology (R)
Herlev Ringvej 75
Herlev 2730
Denmark

Skogholt Peter
Medical Physics
Vejle Sygehus
Kabbeltoft 25
Vejle 7100
Denmark

Skretting Arne
Dept of Medical Physics
Rikshospitalet-Radiumhospitalet
Montebello
Oslo 310
Norway

Spanne Oddvar
Stråleterapi
UNN
Boks 13
Tromsø
Norway

Spejlborg Harald
Dept. of Medical Physics
Aarhus University Hospital
Noerrebrogade 44
Aarhus 0
Denmark

Strickert Trond
Kreftavdelingen
St. Olavs Hospital
Olav Kyrres gt
Trondheim
Norway

Sylvarnes Rune
Stråleterapi, Kreftavd.
Universitetssykehuset Nord-Norge
Kreftavd., P.b. 17
Tromsø 9038
Norway

Søndergaard Jimmi
Oncology
Aarhus University Hospital
Nørrebrogade 44 , byg 5
Aarhus 8000
Denmark

Sørensen Thomas Sangild
Dept Computer Science and Inst. Clinical Medicine, University of Aarhus
Aabogade 34
Aarhus N 8200
Denmark

Søvik Åste
Department of Radiation Biology
Rikshospitalet University Hospital
Montebello
Oslo 310
Norway

Tanderup Kari
Dept. of Oncology
Aarhus University Hospital
Noerrebrogade 44
Aarhus 8000
Denmark

Tanyi James
Radiation Medicine
Oregon Health & Science University
3181 SW Sam Jackson Park Rd
Portland, OR 97239
USA

Taschner Anja
Sales
IBA Dosimetry
Bahnhofstr. 5
Schwarzenbruck 90592
Germany

Thomsen Mette Skovhus
Medical Physics
Aarhus University hospital
Noerrebrogade 44
Aarhus 8000
Denmark

Toma-Dasu Iuliana
Department of Medical Radiation Physics
Stockholm University and Karolinska Institutet, Box 260
Stockholm
Sweden

Tomaszewicz Andrej
Radiofysik
Universitetssjukhuset i Lund
Klinikgatan 7
Lund
Sweden

Uhrdin Johan
Research
Raysearch Laboratories AB
Sveavägen 25
Stockholm 11134
Sweden

Valentini Vincenzo
Radiotherapy Department
Università Cattolica S.Cuore
Roma
Roma
Italy

Vallhagen Dahlgren Christina
Hospital Physics, Oncology, Radiology and Clinical Immunology
Akademiska Sjukhuset
Uppsala 75185
Sweden

van Herk Marcel
Division of Radiotherapy
Netherlands Cancer Institute - AvL
Plesmanlaan 121,
Amsterdam
The Netherlands

Verellen Dirk
Department of Radiotherapy, Oncology Center, Academic Hospital, Vrije Universiteit Brussel
Laarbeeklaan 101, Brussels
Belgium

Vestad Tor Arne
Department of Medical Physics
the Norwegian Radium Hospital
Ullerch. 70
Oslo 310
Norway

Vestergaard Anne
Afd. for Medicinsk fysik
Århus Sygehus
Nørrebrogade 44
Århus C 8000
Denmark

Vikström Johan
KBK-avdeling stråleterapi
Stavanger Universitetssjukehus
Postboks 8100
Stavanger 4068
Norway

Vilarino-Varela Maria
Radiotherapy
St Bartholomew
25 Bartholomew
London
United Kingdom

Ward Lennart
BU Nordic
Elekta Instrument AB
P.O. Box 7593
Stockholm
Sweden

Wasilewska Hanna
Department of Oncology
Vejle Sygehus
Kabbeltoft
Vejle 7100
Denmark

Wersäll Peter
Dpt . Gen Oncology
Radiumhemmet,
Karolinska Universitets Sjukhuset,Solna
Stockholm
Sweden

Widder Joachim
Radiotherapy
UMC Groningen
Hanzeplein 1
Groningen
Netherlands

Wikström Kenneth
Sjukhusfysik
Oncology, radiology, clinical immunology
Akademiska Sjukhuset
Uppsala 0
Sweden

Wright Pauliina
Dept of Medical Physics, Dept of Oncology
Aarhus University Hospital
Nørrebrogade 55, building 5
Århus C 8000
Denmark

Wunderink Wouter
Radiotherapy
Erasmus MC - Daniel den Hoed cancer center, Groene Hilledijk 301
Rotterdam
the Netherlands

Wysocka Barbara
Department of Oncology
Aarhus University Hospital
Nørrebrogade 44
Århus 8000
Denmark

Wåhlin Erik
Department of Hospital Physics
Karolinska University Hospital
Radiumhemmet P8:02
Stockholm
Sweden

Zhang Sean
Radiation Physics
MD Anderson Cancer Center
1515 Holcombe Blvd., Unit 1210
Houston 77030
USA

Ølberg Ståle
Kreftsenteret
UUS
Kirkeveien 166
Oslo 407
Norway

Ørum-Petersen Lene
Radiologisk afd
Aalborg sygehus, ass
Hobrovej 18-22
Aalborg 9100
Denmark

Østergaard Leif
Center of Functionally Integrative
Neuroscience
Aarhus University Hospital
44 Norrebrogade
Aarhus 8000
Denmark